LCGC
solutions for separation scientists
An *LCGC* e-book • November 2013
www.chromatographyonline.com

FIVE KEYS TO SUCCESSFUL GAS CHROMATOGRAPHY

ADVANSTAR SCIENCE

LCGC
solutions for separation scientists
An *LCGC* e-book • November 2013

FIVE KEYS TO SUCCESSFUL GAS CHROMATOGRAPHY

Cover Design:
Rajesh Thangappan

Art Direction:
Dan Ward

Five Keys to Successful Gas Chromatography

Gas chromatography (GC) benefits greatly from certain best practices, as do other scientific disciplines. At the top level these practices might fall into three categories: routine maintenance procedures that help prevent problems, troubleshooting and rescue procedures for resolving new problems, and systematic ways to go about improving routine operations to meet new requirements or enlist new technologies. The most interesting practices lie in the second category, because these are the problems that plague chromatographers the most and impart the highest level of immediate impact. The first and third are not wisely neglected, either. Preventive maintenance mitigates the inevitable onset of problems. Adopting new technologies and requirements helps improve some or all of the sensitivity, accuracy, precision, cost, and time metrics that laboratories run by.

This e-book includes five selections from the "GC Connections" archives that address these key issues. A summary of recommended preventive maintenance procedures for GC gives guidelines for minimizing the chances for an easily avoidable problem. Three specific problem-solving discussions address some common situations with practical descriptions and recommended solutions. Finally, considerations for incorporating higher-speed chromatography and hydrogen carrier gas round out this collection.

The author and the editors of *LCGC* magazine hope that readers will find the selections useful and instructive.

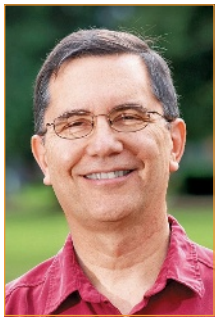

John V. Hinshaw is a Senior Scientist at BPL Global, Ltd., in Hillsboro, Oregon, and a member of *LCGC*'s editorial advisory board. Direct correspondence about this column to the author via e-mail: lcgcedit@lcgcmag.com.

Super Clean™ Gas Filters

with Electronic Indicator

new ***'Talking' Filters!***

Fast Stabilization
Helium Filled GC/MS Triple Filter

Traditional Indicators
Uses sensitive color changing indicators to identify leaks or other system failures which can cause pre-mature saturation

Compatibility
New **Universal** Ring Nut. Easier Installation and improved compatibility with other base plate systems

Electronic Indicator
Progressively displays real-time filter status instead of a 'last minute' color change from traditional indicators, allowing you to determine a more controlled replacement schedule for your installation to prevent unexpected downtime

New Universal Ring Nut

- Serves as a **mounting point** for the Electronic Indicator device
- Easier attachment of genuine SGT purifiers to **competing** base plate systems.
- Can be used to **retrofit** (competing) filters with an electronic indicator
- **Backwards** compatible

Electronic Indicator

- Audio-visual **early warning** system
- Enjoy **additional replacement filter discounts** when filter is replaced according schedule
- Can be **linked** to our virtual indicator platform or can be **manually** configured according your replacement schedule preferences.

www.virtualindicator.com/preorder

For more information go to www.virtualindicator.com - Pre-ordered items are targeted to be shipped November 2013

Peak Problems

How to handle partially resolved or distorted peaks that yield poor quantitation

The goal of quantitative chromatography is to separate two or more substances sufficiently so that they can be measured with a desired degree of accuracy and precision. The resolution of a peak pair provides a standardized measurement of the extent of a separation, but strictly speaking, resolution is defined only for two Gaussian peaks of equal size. Below, we first discuss resolution and the effects that relative peak size have on area measurements. Then we examine the effects of peak tailing on resolution and peak overlap. Finally, we test the quantitative area measurement of a pair of tailing peaks and examine some alternative measurements of the goodness of peak resolution.

Resolution

The resolution of a pair of adjacent peaks is defined in the chromatographic literature and in standard nomenclatures such as IUPAC (1) or ASTM E355 (2) as follows:

$$R_s = 2.0(t_{R2} - t_{R1})/(w_{b2} + w_{b1}) \quad [1]$$

For a Gaussian-shaped peak the width at half-height is related to the width at base by a factor of 1.699:

$$w_b = 1.699 \times w_h \quad [2]$$

It is usually more convenient to calculate resolution from the width at half-height of the second peak using this related formula:

$$R_s \approx (t_{R2} - t_{R1})/(1.699 w_{h2}) \quad [3]$$

The width at half-height is more easily measured than the width at base, and it is measured and used by many chromatography data-handling systems in, for example, system suitability calculations. The width of the second peak is used because it generally will be either equal to or slightly greater than the first peak's width and thus, produces a more conservative result while not requiring measurement of the widths of both peaks.

Most chromatographers are familiar with the appearance of partially resolved, baseline resolved, and fully resolved peak pairs. Figure 1 shows an ideal pair of generated Gaussian peaks of equal sizes and widths with partial resolution at R_s = 1.0 (Figure 1a), baseline resolution at R_s = 1.5 (Figure 1b), and full resolution at R_s = 2.0 (Figure 1c). In this illustration, resolution increases as the separation between the peaks increases, while the same peak shape is maintained. Keeping the same separation while decreasing the peak widths also would increase their resolution proportionately. Figure 1c illustrates the relationship between the peak width at half-height and base, and it also shows how the width at base is determined from the baseline intersection points of lines drawn tangent to the peak's upward and downward slopes. A common misconception is that the width of a peak at base is the time between when the peak starts to rise above the baseline until it subsides back into the baseline — the peak integration start and stop times — but in fact, the base width of a Gaussian peak is measured at 13.4% of the peak height above the baseline, at the times corresponding to the tangent–baseline intersection points.

Table I lists the retention times, peak width measurements, and resolution for the three cases shown in Figure 1.

At resolution of 1.0 the valley point between the peaks corresponds with the end of the first peak's base width and the start of the second peak's base width. At baseline resolution, where R_s = 1.5, the ending and starting base widths of the first and second peaks, respectively, are separated by 0.5 times the base width. At resolution 2.0, the ending and starting base widths of the first and second peak are each spaced at intervals equal to the base width.

Peak Identification: The identification of specific peaks by their retention times becomes more certain as resolution increases. It is possible to identify peaks on the basis of a partial separation, but the certainty of identification improves with increasing resolution. The detector signal comes closer to baseline between the peaks and the presence of additional components becomes more apparent. A mass-selective detector helps to identify merged peaks on the basis of their mass spectra, but closely eluted peaks often are isomeric or otherwise chemically similar. They may have similar spectra that preclude unambiguous identification by spectral library matching.

Each component in a group of two or more merged peaks should be identified with separate analyses of the pure components, and the influence of matrix components should be determined through blank injections. Bear in mind, too, that the elution order

Table I: Resolution measurements from Figure 1. The callouts to (a), (b), and (c) refer to the parts of Figure 1.

Both Peaks			Peak 1	Peak 2	Δt_R (s)	R_s
w_b (s)	w_h (s)	σ (s)	t_{R1} (s)	t_{R2} (s)		
16	9.42	4	200	216	16 (4σ)	1.0 (a)
				224	24 (6σ)	1.5 (b)
				232	32 (8σ)	2.0 (c)

Table II: Peak area measurements from Figure 1. Overlap is the amount of area or percentage of one peak into the other. The callouts to (a), (b), and (c) refer to the parts of Figure 1.

Both Peaks				
Known Area (μV-s)	Resolution	Measured Area (μV-s)	Overlap Area (μV-s)	Percent Overlap
15,000	1.0 (a)	14,970	349	2.33%
	1.5 (b)	14,997	21.4	0.14%
	2.0 (c)	14,979	<0.1	~ 0.0%

Figure 1: Resolution and measurement of a pair of identical Gaussian peaks. Peak 1: green dotted line. Peak 2: red dotted line. Chromatogram: blue solid line. Overlapping area of peak 2 inside peak 1: red shaded area. Overlapping area of peak 1 inside peak 2: green shaded area. (a) Resolution = 1.0; (b) resolution = 1.5, inset shows extent of peak overlap; (c) resolution = 2.0, dotted grey lines show tangents to the peaks and measurement of width at base.

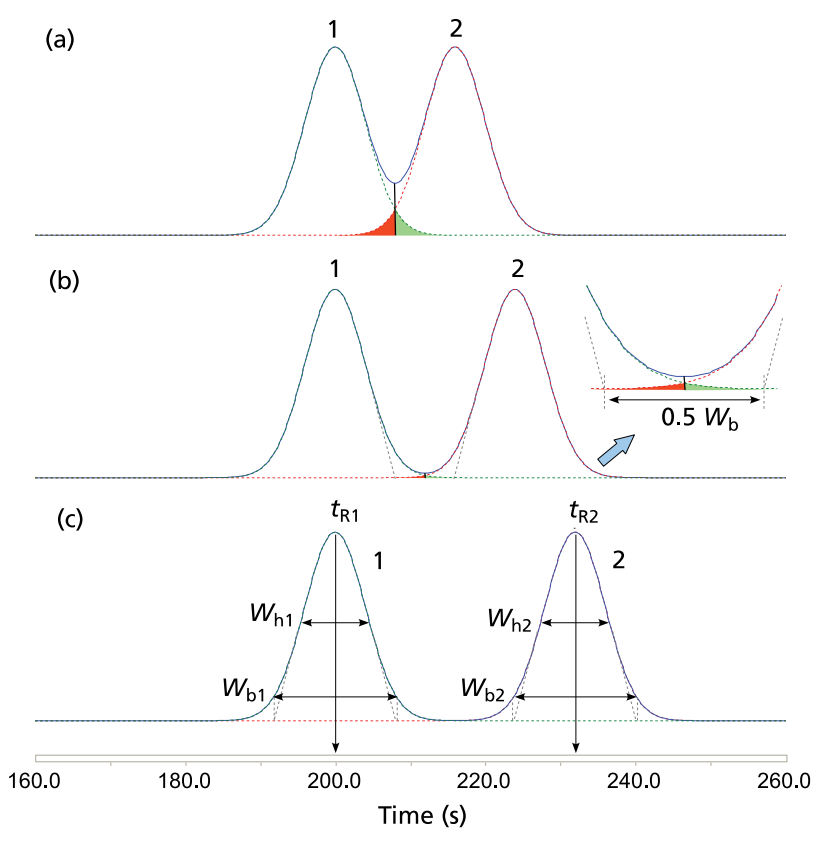

of close peaks will be influenced by changes in the column temperature conditions: a change in temperature program rate of as little as 2 °C/min can reverse elution order. When faced with the partial resolution of a critical peak pair, or with the presence of a new matrix compound that interferes, make sure that the current separation conditions are optimal and then consider upgrading the column resolving power by installing a longer or narrower-bore column. If all else fails, then try changing to a different stationary phase that better separates the peaks of interest.

Quantitative Analysis: Measurement of a partially resolved peak pair can be difficult to achieve with acceptable levels of accuracy. The simple but unrealistic case of two equal-sized peaks is a good starting point for understanding the effects that colliding peaks have on quantitative analysis. Both the influence of the portion of one peak that extends into another and the effects that merged peak shapes have on peak integration play strongly into the accuracy of quantitative measurement of merged peaks.

Returning to Figure 1, the degree of area overlap of the coinciding portions of the peaks decreases as resolution increases. At R_s = 1.0 in Figure 1, the contribution of either peak to the other's total area is about 2.3%, as measured from where a vertical dividing line for peak area integration is dropped from the valley point between the two peaks to the baseline. I measured the overlap areas with a measurement tool in my data system for the first generated peak alone by starting at the time of the valley point, which corresponds with the end of the peak's w_b segment, and extending to the end of the peak. In this case, the peaks are symmetrical and identical so the overlap and total areas are the same for each.

The overlapping areas are highlighted in color in Figure 1a and in the inset in Figure 1b. As the

Table III: Peak areas and overlap of unequal peaks. Overlap is the amount of area or percentage of one peak into the other. The callouts to (a), (b), and (c) refer to the parts of Figure 2.

R_s	Peak 1				Peak 2			
	Known Area (µV-s)	Measured Area (µV-s)	Overlap Area (µV-s)	Percent Overlap	Known Area (µV-s)	Measured Area (µV-s)	Overlap Area (µV-s)	Percent Overlap
1.0 (a)	150,000	151,476	2056	1.36%	15,000	13,448	296.7	2.21%
1.5 (b)		150,033	97.1	0.06%		14,958	45.9	0.31%
2.0 (c)		150,000	0	0%		14,997	0	0%

Table IV: Influence of integration type on areas of partially resolved unequal peaks R_s = 1.0. The callouts to (a), (b), and (c) refer to the parts of Figure 3.

Integration	Peak 1			Peak 2		
	Known Area (µV-s)	Measured Area (µV-s)	Percent Error	Known Area (µV-s)	Measured Area (µV-s)	Percent Error
Valley (a)	150,000	151,476	0.98%	15,000	13,448	−10.3%
Tangential skim (b)		156,750	4.5%		5617	−62.6%
Exponential skim (c)		151,500	1.0%		10,425	−30.5%

Figure 2: Resolution of peaks of unequal size. The peak widths and separations are the same as in Figure 1. The area of peak 1 is 10 times the area of peak 2.

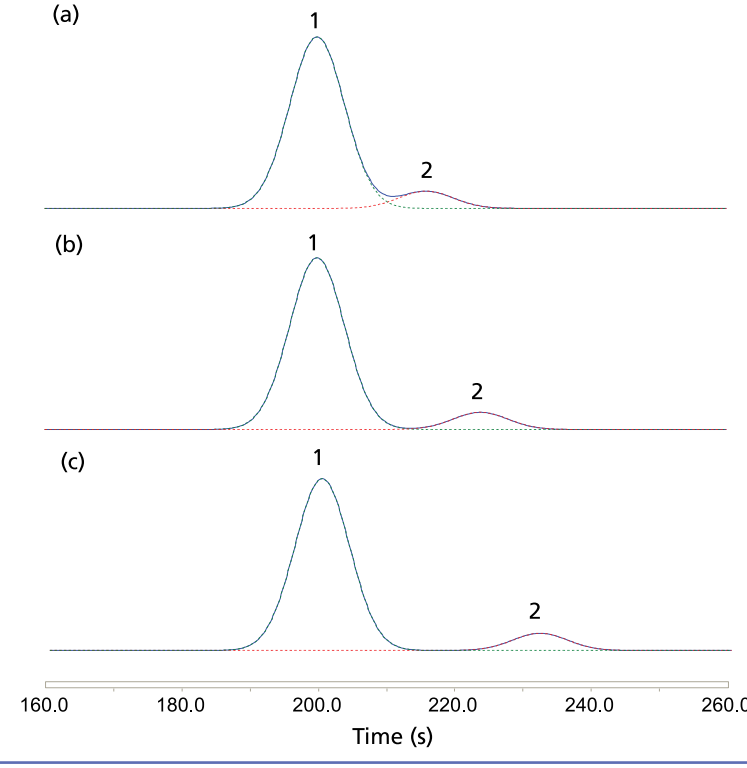

resolution increases to 1.5 — baseline resolution — the overlap between the two peaks drops toward 0.1%, and at a resolution of 2.0 no measurable overlap remains. Table II gives the area measurements from Figure 1. The values for each peak are very close to the known areas as set when the peaks were generated.

In this idealized situation, there is no significant error between the measured and known peak areas, even down at a resolution of 1.0. However, real peaks are not equal in area and width because their amounts, detector response factors, and shapes vary. Also, real-world peaks incorporate uncertainty in their measurement due to injection variability, detector noise, and slight shifts in retention time from run to run. It is instructive to consider what happens when one peak is considerably larger than the other and what the effects imply about the influence of peak resolution on quantitative analysis.

Unequal Peak Sizes

Increasing the size of the first peak in our example affects both the peak separation and area measurements. The disparity in peak sizes changes the degree of peak overlap, but more significantly, it has a profound effect on quantitative measurements. Figure 2 shows the same three cases as in Figure 1, but the first peak is now 10 times larger. A question arises of whether the classical resolution measurement, which is based upon two equal-sized peaks, is applicable when the peak sizes are significantly different.

We can use the degree of area overlap between the peak pair as an indicator of the degree of peak resolution, and compare the case of equal-sized peaks to that of unequal peaks. Looking first

Figure 3: Influence of integration type on the measured areas of unequal peaks. Peak pair with R_s = 1.0 from Figure 2a. (a) Vertical drop from valley to baseline. (b) Tangential skim underneath the second peak. (c) Exponential skim off the first, larger peak. The insets show the baselines in more detail.

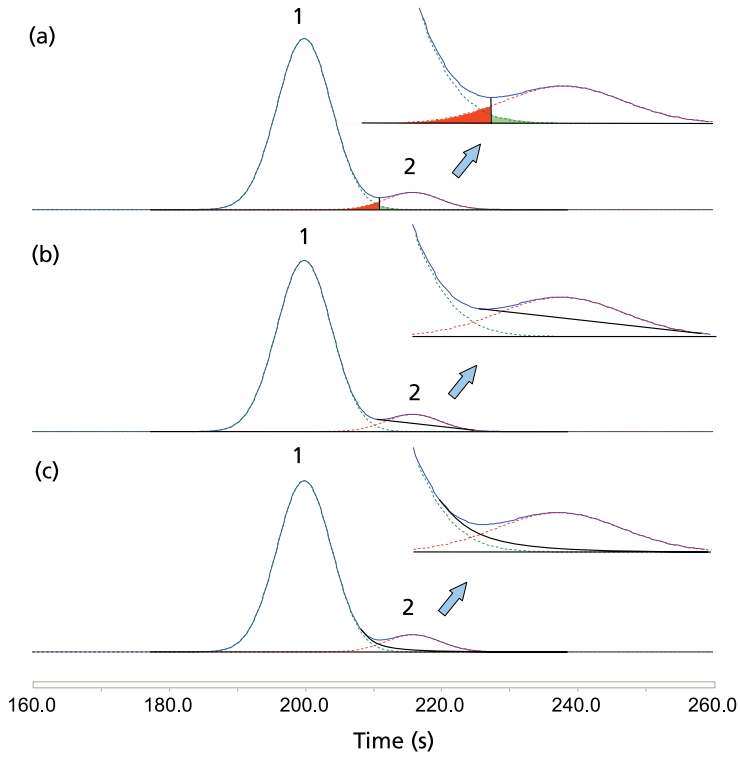

Figure 4: Peak measurements for calculation of resolution. Peak 1 and peak 2 are identical nontailing Gaussian peaks with σ = 4.0 s and τ = 0.0 s. The peaks are spaced 8σ apart (32 s), and R_s = 2.0.

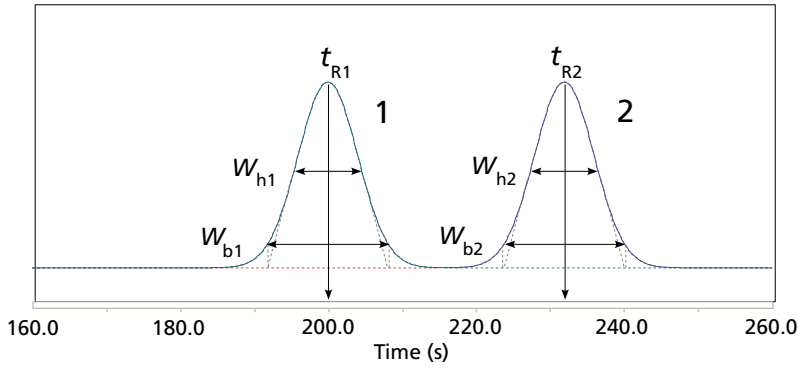

at Figure 2a (the case of partial resolution of 1.0 of peaks with a size ratio of 10:1), the first peak's percentage of overlap into the second, as listed in Table III, is similar to that of a pair of equal-sized peaks when there is a simple vertical division between the two peaks at the valley point. In the case of baseline resolution, in Figure 2b, Table III lists the overlap of the larger first peak into the smaller second peak at 0.31% of the second peak's area, while the second peak's overlap into the first is only 0.06%.

The overlap for the unequal peaks is small and similar to the degree of overlap of 0.14% for a pair of equal-sized peaks, so the definition of the resolution of equal-sized peaks seems to extend to at least at a peak area ratio of 10:1. In the case of resolution equal to 2.0, in Figure 2c, there is no measurable influence of either peak on the other: they are indeed fully resolved and independent.

Quantitative area measurements in the case of baseline or better resolution of unequal peaks are fairly accurate. The measured and known areas in Table III for cases of baseline resolution (Figure 2b) and full resolution (Figure 2c) compare very well. Going from a 1:1 area ratio to a 10:1 area ratio with a pair of peaks at baseline resolution or better should yield a nearly linear trend between peak size and measured area. At some point, as the area ratio increases above 10:1, however, the degree of influence of the larger peak on the smaller one's measured area will become significant and the linear relationship between peak size and measured area will break down. Greater resolution between the peaks will raise this ceiling on linearity.

At a partial resolution of R_s = 1.0, the story is quite different. Now, there is a much larger overall error in measured area counts with a peak size ratio of 10:1, which was not hinted at when only the similar degree of area overlap for equal and nonequal peak sizes was considered. Not surprisingly, the largest errors occur for the smaller peak.

The error level depends strongly on the type of baseline allocation selected for the data system. Figure 3 illustrates three common choices. First is a simple vertical separator dropped from the valley point to the baseline, which we have used throughout this discussion thus far, shown in Figure 3a. This choice produces an error of about +1% for the larger

Table V: Peak measurements from Figure 5. Measurement of A_s is at 10% of peak height (2).

Figure	σ (s)	τ (s)	w_h (s)	w_b (s)	w_b/w_h	A_s (s)
5a	4	0	9.5	16.1	1.70	1.0
5b	4	4	11.6	20.0	1.72	1.4
5c	4	8	14.4	25.0	1.74	2.1

Table VI: Retention times to attain specified resolution for equal-size peaks. The symmetrical peaks are those shown in Figure 5a, and the tailing peaks are those shown in Figure 5b. The data on symmetrical peaks are from the first part of this chapter. The callouts to (a), (b), and (c) refer to the parts of Figure 6.

Resolution	Retention Time of Symmetrical Peaks		Retention Time of Tailing Peaks	
	Peak 1	Peak 2	Peak 1	Peak 2
1.0	200.0	216.0	200.0 (a)	220.3 (a)
1.5	200.0	224.0	200.0 (b)	229.6 (b)
2.0	200.0	232.0	200.0 (c)	239.4 (c)

Table VII: Peak area measurements from Figure 6. Overlap is the percentage of the area of one peak that extends into the other. The data on symmetrical peaks are from the first part of this chapter. The peaks all have the same area. The callouts to (a), (b), and (c) refer to the parts of Figure 6.

Resolution	Percent Overlap of Symmetrical Peaks		Percent Overlap of Tailing Peaks	
	Peak 1	Peak 2	Peak 1	Peak 2
1.0 (a)	2.33%	2.33%	5.75% (a)	1.29% (a)
1.5 (b)	0.14%	0.14%	1.19% (b)	0.16% (b)
2.0 (c)	~ 0.0%	~ 0.0%	0.17% (c)	0.02% (c)

peak, while the smaller peak comes back with an area that's about 10% smaller than the known amount, as listed in the first line of Table IV. This effect is seen graphically in the inset of Figure 3a, where the relative amount of the second peak that's overlapped into the first is a significant fraction of the second peak's size.

A tangent skim baseline choice puts a straight line at the valley point and tangential to its intersection with the declining side of the smaller peak. When a tangent skim is selected, the error in the second peak's area becomes unacceptably huge at −63%. This effect is visualized easily by examination of the inset in Figure 3b, where a very large portion of the second peak is lost into the area of the first. This shift of area also biases the first peak's area upward by 4.5%.

Finally, using an exponential skim or curve fit off of the first peak reduces the error relative to the tangent skim, but for the second peak the loss of area is still very large at −31%. Looking at the inset in Figure 3c, the curve-fit of the exponential skim to the first peak is fairly good and overestimates the peak size by only 1%. The loss of a significant portion of the second peak is obvious.

The errors associated with these three different baseline allocation choices depend on the relative sizes of the peaks and their resolution. What I've shown here is just a snapshot of one artificial situation. Chromatography data-handling systems include conditional code that allows users to select boundaries for cases in which different baseline allocations are to be applied, based upon relative peak heights, valley points, and other parameters. This means that the choices for baseline allocation must be made carefully and validated across the entire targeted range of analyte concentrations.

Symmetrical-Peak Resolution: Conclusions

The resolution of a pair of Gaussian chromatographic peaks provides a useful metric for gauging the ability to achieve reliable qualitative peak identification as well as predicting the accuracy of area measurement. As long as peak resolution is at baseline or better levels, quantitative errors can be very low, even for adjacent peaks at size ratios up to 10 to 1. When the resolution falls below the baseline level, the measurement of peak areas becomes difficult. Careful choices for area integration in data-handling systems can minimize the errors, but must be checked across the entire operating range of a method. Selecting conditions and columns that better resolve critical peak pairs can be a better choice than relying upon the data system's rules of area integration to slice away partially resolved peaks from each other.

Peak Tailing and Peak Overlap

As a reminder, in equation 3 t_R is the retention time, w_b is the peak width-at-base as measured at 13.4% of the peak height, and w_h is the peak width at it's half-height. The subscript numbers indicate which peak. Measurements of the peak retention times and widths for the purposes of determining resolution are shown in Figure 4 for a pair of peaks with $R_s = 2.0$.

These relationships are cast in terms of a pair of identical symmetrical peaks, but the definition of resolution does not limit the relative sizes of the peaks or their shapes. Resolution calculations are performed routinely on pairs of peaks that can be quite different in size and shape, yet the effects of disparities in peak

Figure 5: Exponentially modified Gaussian (EMG) peak model. Three peaks with increasing tailing and identical areas and retention times (peak apex): (a) symmetrical Gaussian peak with $\sigma = 4.0$ and $\tau = 0.0$, the same as in Figure 4; (b) same as peak 1 with $\tau = 4.0$; (c) same as peak 1 with $\tau = 8.0$.

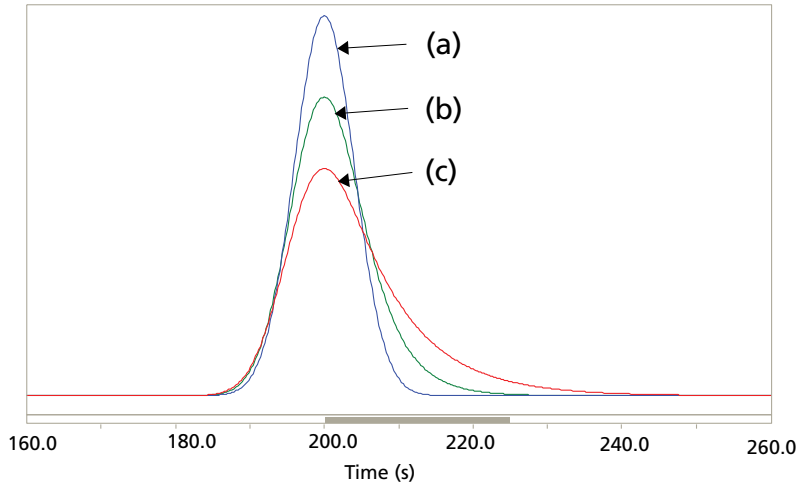

Figure 6: Resolution and overlap of tailing peaks. Peak shapes as in Figure 5b. Resolution: (a) 1.0, (b) 1.5, (c) 2.0.

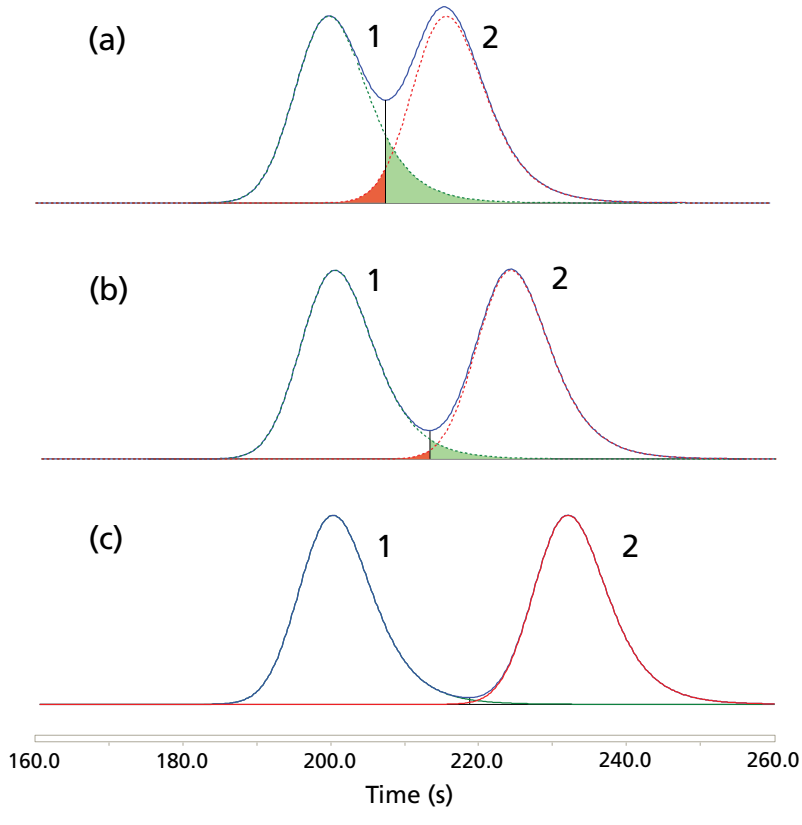

shapes on quantitative measurements are rarely assessed. The preceding sections of this chapter demonstrate that increasing the size of the first peak up to 10 times the size of the second did not materially affect quantitative measurements, as long as the peak resolution was at the "baseline" level of 1.5 or greater and a simple vertical peak boundary at the valley point — I'll call this method valley integration — delineated the first peak from the second. With a less-than-baseline resolution of 1.0, however, where the difference in the retention times of symmetrical peaks is equal to the average of their widths at base, significant measurement errors of up to 10% for the smaller peak's area were incurred for valley integration. Even greater errors were caused by either tangential or exponential skimming methods of peak integration. Thus for this limited set of examples, a requirement that symmetrical peak pairs have resolution of 1.5 or greater is well justified.

Nonsymmetrical Peaks

In reality, chromatographic peaks are not truly Gaussian in nature. This symmetrical peak shape arises from purely theoretical and idealized treatments of mechanisms of retention and transport through a chromatographic system. As soon as significant dead volumes, adsorption, nonlinear mass transfer, thermal gradients, or other real-world effects occur, peak shapes depart from the ideal. Non-Gaussian peak profiles, tailing or fronting peaks, and other distortions are the rule rather than the exception. Of these, peak tailing is perhaps the most commonly encountered effect. Tailing can be simulated by the convolution of a Gaussian peak profile with an exponential decay function. Granted, this technique takes idealized symmetrical peaks and adds idealized peak tailing, and so does not represent real-world peaks any better than the purely Gaussian shapes, but it comes close and it certainly provides a useful model for discussion.

Figure 5 illustrates the effect on a Gaussian peak of imposing increasingly stronger peak tailing. The degree of peak tailing

Table VIII: Area measurement of partially resolved tailing peaks. Peak 1 is 10× larger than peak 2; both have asymmetries of 1.4. The appearance of the peaks at resolution = 1.0 is illustrated in Figure 7, to which the letters (a), (b), and (c) refer.

Resolution	Peak Number	t_R (s)	Known Area	Vertical Drop (a)		Tangential Skim (b)		Exponential Skim (c)	
				Measured Area	% Error	Measured Area	% Error	Measured Area	% Error
1.0	1	200.0	150,000	146,292	-2.5%	159,363	6.2%	152,669	1.8%
	2	220.3	15,000	15,473	3.2%	3152	-79.0%	9846	-34.4%
1.5	1	200.0	150,000	147,060	-2.0%	152,064	1.4%	148,395	-1.1%
	2	229.6	15,000	15,455	3.0%	10,451	-30.3%	14,120	-5.9%
2.0	1	200.0	150,000	147,596	-1.6%	148,718	-0.9%	147,816	-1.5%
	2	239.4	15,000	14,918	-0.5%	13,721	-8.5%	14,698	-2.0%

Figure 7: Influence of integration method on the measured areas of unequal sized asymmetrical peaks. Peak pair with R_s = 1.0 (a) Vertical drop from valley to baseline; (b) tangential skim underneath the second peak; (c) exponential skim off the first, larger peak.

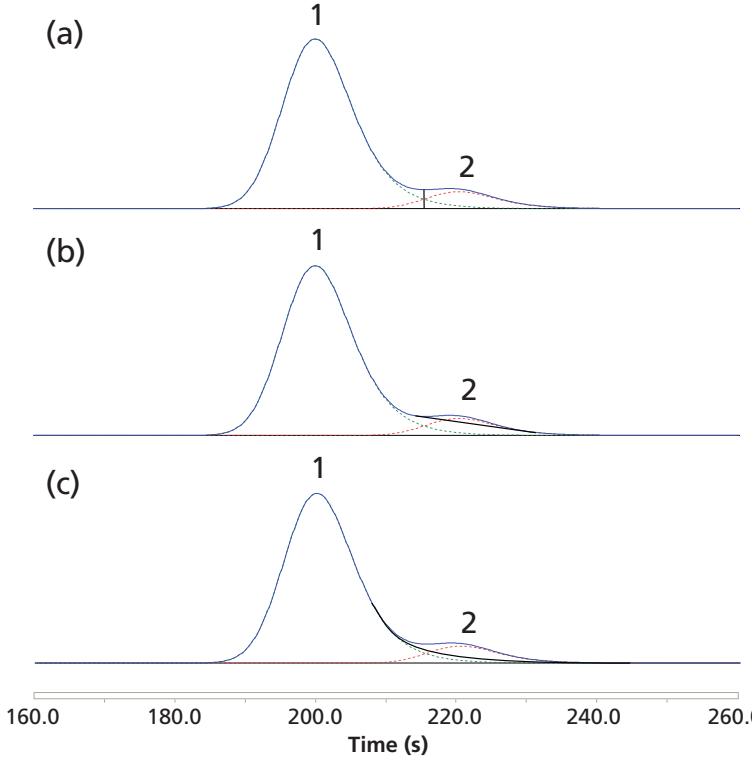

is determined by an exponential decay factor τ, sometimes referred to as the *exponential time constant*, using an exponentially modified Gaussian peak mathematical model (3). Figure 5a shows a purely Gaussian peak, Figure 5b shows the effect of an exponential decay factor τ equal to the peak's standard deviation σ, and Figure 5c shows an exponential decay factor of twice the standard deviation. From experience, most gas chromatographers would agree that peaks which lie between the purely symmetrical shape of Figure 5a, where the asymmetry factor A_s = 1.0, and the slightly tailing shape of Figure 5b, where A_s = 1.4, would be acceptable, while the more strongly tailing peak of Figure 5c, where A_s = 2.1, might be considered as exhibiting excessive tailing. Table V lists measurements of the widths and asymmetry factors for these three peaks. In particular, it is significant that the ratio of the peaks widths at base to the widths at half-height are roughly constant. This implies that we can apply the alternative version of the resolution equation given in equation 3 for determining the resolution of slightly to moderately tailing peaks, with asymmetry factors ranging from 1.0 to 2.0. The measurement of single peak asymmetry and the effects of asymmetry on peak area determination were discussed in two previous "GC Connections" columns (4,5). Now let's consider the effects of peak tailing on the resolution of a pair of peaks with the characteristics of the peak shown in Figure 5b.

Resolution of Tailing Peaks

The resolution of a pair of peaks is defined in terms of their separation and widths. Peak tailing increases the widths of affected peaks, so to maintain a proscribed resolution level, the separation between a pair of peaks must increase in proportion to the amount of peak tailing. Earlier in this chapter, the characteristics of a pair of symmetrical peaks were measured at R_s = 1.0, 1.5, and 2.0. The symmetrical peak retention time data is given here in the first part of Table VI and the peak overlap data is given in the first part of Table VII. These symmetrical peaks have the peak shape from Figure 5a.

For comparison, the second parts of Tables VI and VII show

Figure 8: Measurement of the discrimination factor: (a) peaks of equal height; (b) peaks of unequal height.

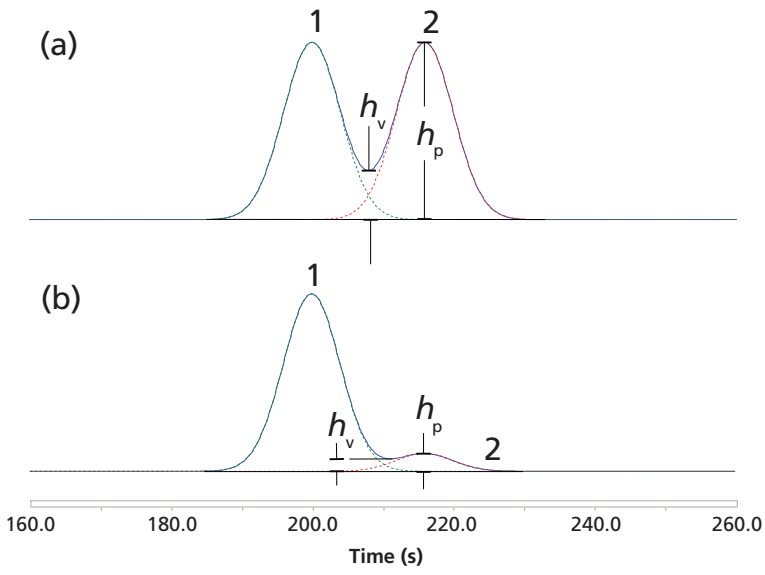

how far apart the asymmetrical peaks must stand to achieve the stated resolution, and to what degree the peaks overlap when a moderate degree of tailing, with A_S = 1.4, is applied to both peaks by using the peak shape from Figure 5b. Looking first at Table VI for the retention data, an increase in the second peak's retention time of 4–7 s is required, depending on the selected resolution level, to maintain the same resolution as peak tailing increases. Thus, considering only the resolution measurement for the moment, it is evident that when designing a robust chromatographic method that anticipates a certain degree of peak tailing, the degree of separation of the peaks must be significantly greater than would be required by accommodating only nontailing peaks.

But now consider the meaning of peak resolution. It is tied directly to the degree of overlap of a pair of peaks. The goal is to provide an acceptable tradeoff between area measurement inaccuracies and the degree of separation. The expectations set by the overlap of symmetrical peaks are listed in the first part of Table VII. Here we can see that the overlap of a pair of symmetrical peaks with resolution of 1.5 is about 0.14%. This low overlap is the desired result of separating peaks at baseline resolution. It is the basis for the familiar guideline that baseline resolution allows for adequately accurate area measurements.

When peaks start to tail, however, this assumption breaks down. The first peak in the pair of tailing peaks under consideration, when separated sufficiently to produce a measured resolution of 1.5, extends into the second peak with an area that is 7.6× greater than is obtained for the pair of symmetrical peaks at the same resolution. At a resolution of 2.0, the overlap area of the first asymmetrical peak into the second is about equal to the degree of overlap for the pair of symmetrical peaks at a resolution of 1.5. Thus, the degree of peak tailing has a direct effect on the meaning of baseline resolution. Higher resolution is required for tailing peaks to achieve the same degree of area overlap as nontailing peaks.

For the development of robust methods, a good guideline is to require the initial resolution of critical peak pairs to be at least 2.0, and preferably higher. Then, as peaks start to tail while columns age or inlets become contaminated with use, there will still be sufficient resolution available to achieve an acceptable separation. Providing a somewhat higher resolution also grants some leeway for drifting retention times due to aging, and it facilitates the acceptability of new columns over the lifetime of a method as column manufacturers' normal variabilities come into play.

Peak Tailing and Peak Overlap: Conclusions

Now we have characterized the behavior of symmetrical and nonsymmetrical peaks in terms of the effects of peak tailing on measured resolution and area overlap between peak pairs. For the moderately tailing peaks examined, greater differences in retention time are required to achieve a given resolution compared to symmetrical peaks, as might be expected. But the degree of overlap from the first peak into the second peak is greater for tailing peaks than for symmetrical peaks at the same resolution level, so additional resolution is required to achieve baseline separation of tailing peaks. Now, let's examine the effects that peak tailing has on measured areas and take a look at some metrics other than resolution for characterization of the quality or degree of separations.

Accurate Peak Area Measurement

When peaks tail, even moderately, extra time between them is required to attain the same resolution as for nontailing peaks because of the overall increase in peak widths caused by tailing. Even when the same resolution is attained, however, the degree of area overlap between tailing peaks is greater than for nontailing peaks, and more so for the amount of excursion of the first peak into the second. Thus, additional resolution is required for tailing peaks to achieve the same degree of peak area overlap as

a pair of nontailing symmetrical peaks.

The amount of area overlap of one peak into another can be measured as the percentage of a peak's area that lies underneath the adjacent peak, where the peaks are separated with a specific degree of resolution, as explained in previous sections of this chapter. In that case, where the peaks were of equal size, resolution of 2.0 was needed to bring the degree of overlap of a first tailing peak into the second down to about the same level seen with symmetrical peaks at resolution of 1.5, at around 0.5%. This was despite the moderate increase in peak separation required to keep the measured resolution the same for tailing peaks as for nontailing ones.

The degree of peak overlap can be calculated easily enough with the theoretical peak model being used here, but it isn't a realistic measurement of the effects that less-than-ideal peak separation has on actual area measurement of peaks that are coeluted in a chromatogram. With nonselective detectors, it isn't possible to measure the two peaks independently, as was done here to obtain the degree of overlap. Even with a mass spectrometer or other selective detector, there often isn't sufficient selectivity to obtain 100% discrimination between overlapping peaks, so questions of the effects of peak overlap on quantitative measurements are not answered by overlap calculations.

In some cases, mathematical peak deconvolution can be used to tease apart two partially merged peaks, but practically speaking, for routine applications, we have to fall back on the integration parameters available in chromatography data processing systems. To test how well merged tailing peak areas are estimated, I exported a series of synthesized chromatograms with moderately tailing peaks using asymmetries (A_S) of 1.4 in which the peak resolution was set at 1.0, 1.5, and 2.0. Three common peak integration methods were selected for the estimation of peak areas: a vertical drop from the valley point between the peaks down to the baseline; a tangential skim drawn from the valley out to the downsloping side of the second peak; and an exponential skim underneath the second peak. Somewhat unrealistically, no noise was added to the generated peaks, but in this case, I was more interested in the measurements themselves and not the degree of uncertainty across multiple measurements. These results show how one particular data processing system performed. Others would vary, but I expect they might produce very similar results.

Table VIII enumerates the results of this tailing peak faceoff, and Figure 7 shows what the separations looked like at resolution = 1.0. As was the case with symmetrical peaks, increasing peak separation and resolution improved the accuracy of the area measurements significantly. And the influence of the area determination method influenced the measurements in much the same manner. The best results were obtained with a simple vertical drop from the valley between the peaks to the baseline below; the measured values had less than a 4% error in all cases. The exponential skimming technique performed well except for the second, smaller peak when the resolution was less than 1.5. In this case, the error went from about 6% up to nearly 35%. The tangential method delivered a comparably large error of over 8% for the second of two relatively well-separated peaks, and it produced very large errors for the second peak in the cases of the less-resolved peak pairs.

Overall, at resolution 1.0, the valley baseline error for the second, smaller peak was actually somewhat less for the unequal-sized tailing peaks than for the symmetrical peaks, due perhaps to the slightly larger separation of the tailing peaks, while errors for the tangential and exponential methods were consistently larger with unequal-sized tailing peaks than for symmetrical ones. This seems to say that the increased separation between tailing peaks that was required to maintain a degree of area overlap originally seen with nontailing peaks is insufficient to reduce peak area integration errors to similar levels in both cases.

Another observation gave me second thoughts about peak integration in these situations. In the default state, chromatography data handling software has a number of settings that control various automatic thresholds for the onset of exponential skimming versus the vertical drop or other integration methods. These settings were left at their default values for this short study, which caused the automated selection of the area measurement method to change from a vertical drop in the case of resolutions equal to 1.5 and 2.0 to the exponential skim method at resolution of 1.0. The result was a sudden "automatic" decrease in the second peak's area when the resolution dropped off to 1.0, as determined without any intervention, a change that would have resulted in a –34.4% error if the system were allowed to run unobserved. As it was, I forced the use of the vertical drop method to observe its effects. Although I did not explore the effects of changing the relative sizes of the peaks to values other than 1:1 and 10:1, changes in peak size also can trigger unintended shifts in the integration method selected automatically by any data handling system. Therefore, in low-resolution situations, careful examination of the results over the entire range of intended magnitudes of all affected peaks, both analyte and matrix components, must be performed while taking positive control of the integration settings.

Measurements Related to Resolution

The aforementioned issues with peak area determination and resolution arise partially from the fact that peak resolution does not depend upon the relative sizes of

the peaks. Thus, even though the area measurements of two peaks of equal size, tailing or not, can be quite different compared to measurements of two peaks of significantly different sizes, the resolution of the two pairs of peaks is identical: it depends only upon the peak widths measured at base, or on the widths at half-height — as are sometimes easier to measure — converted to base widths.

A number of measurements related to resolution have been described in the chromatography literature, including the peak capacity, which is the number of additional peaks of a specified resolution that could fit between two well-separated peaks. For example, if two peaks have resolution R_S = 6, then three additional peaks of the same width would fit between them if the added peaks were spaced exactly evenly in-between, for a peak capacity of 3. A similar term, the *effective peak number*, refers to the peak capacity in the special case where the resolution between added evenly spaced peaks equals 1.0. The *separation number*, or *Trennzahl*, uses the peak widths at half-height to calculate the number of peaks that would fit between our well-separated pair with R_S = 1.177 and usually is applied to consecutive members of a homologous series of compounds such as *n*-hydrocarbons in retention index calculations. Details of these measurements can be found in reference 6 as well as in many other chromatography textbooks.

Another resolution-related measurement is of interest to the current discussion. As stated earlier, none of these calculations takes into account the effect of differing peak sizes on peak area overlap and integration errors. The discrimination factor, however, does incorporate peak height and it can be a more meaningful metric for evaluation of these concerns (7). The discrimination factor is related to the separation power originally described by Kaiser (8, see also reference 6 for more information) and is calculated graphically as shown in Figure 8 from the relative heights of the smaller peak and the valley above the baseline.

$$d_0 = 1.0 - (h_v/h_p) \qquad [4]$$

In Figure 8a, the discrimination factor is d_0 = 0.72 in the case of equal-sized symmetrical peaks and in Figure 8b with unequal-sized symmetrical peaks, d_0 = 0.30. In both cases the resolution equals 1.0, but the smaller discrimination factor of the peak pair with a 10:1 height ratio in Figure 8b reflects more accurately the reduced degree of separation available when the peak sizes are significantly different.

In the case of tailing peaks of equal heights at resolution 1.0, the discrimination factor also equals 0.72. The discrimination factor does not distinguish between tailing and symmetrical peaks with the same size and resolution, but remember that the tailing peak pair are separated in time by a few more seconds to keep the same resolution as the nontailing peak pair. In the case of the unequal size tailing peak pair with a 10:1 size ratio (Figure 7a), the discrimination factor drops down to 0.04. Compared to a value of 0.30 for the unequal-sized symmetrical peak pair, the effect of peak tailing on the discrimination factor is dramatic, perhaps even overstated. Nevertheless, the discrimination factor does provide a useful indication of how much a larger peak will affect the quality of separation with an adjacent peak both in terms of the peak size and the presence of peak tailing.

Accurate Peak Area Measurement: Conclusions

The effects of peak size and peak tailing on the degree of area overlap and measured peak areas are significant. Changes in peak separation, resolution, and symmetry strongly affect the accuracy of peak area measurements. Conventional resolution measurements do not take into account the effects of disparities in peak size, nor do they completely accommodate the effects of peak tailing. The peak discrimination factor provides some indication of how well a given separation discriminates adjacent peaks from each other and does take into account the effects of peak size and asymmetry.

Careful evaluation of the data processing and area measurements of disparate, partially merged, or tailing peaks can identify potential pitfalls that can be imposed by changes in concentration, peak retention time drift, and asymmetry incurred as chromatography components age and are replaced.

References

(1) A.D. McNaught and A. Wilkinson, *IUPAC Compendium of Chemical Terminology* (International Union of Pure and Applied Chemistry, Research Triangle Park, North Carolina 27709-3757, USA, 1997).

(2) "ASTM E355-96 (2007) Standard Practice for Gas Chromatography Terms and Relationships," Annual Book of Standards, Vol. 03.06 (ASTM International, American Society for Testing and Materials, Conshohocken, Pennsylvania).

(3) A. Felinger, *Data Analysis and Signal Processing in Chromatography* (Elsevier, Amsterdam, The Netherlands, 1998).

(4) J.V. Hinshaw, *LCGC North America* **27**(3), 232–245 (2009).

(5) J.V. Hinshaw, *LCGC North America* **27**(7), 542–549 (2009).

(6) L.S. Ettre and J.V. Hinshaw, *Basic Relationships in Gas Chromatography* (Advanstar, Cleveland, 1994), pp. 75–83.

(7) M.Z. El Fallah and M. Martin, *Chromatographia* **24**, 115–122 (1987).

(8) R. Kaiser, *Gas-Chromatographie* (Akademische Verlagsgesellschart, Leipzig, 1960), p. 33.

How to Cite This Article:

Please note this chapter is a compilation of three installments of "GC Connections."

J.V. Hinshaw, *LCGC North Am.* **28**(7), 524–529 (2010).
J.V. Hinshaw, *LCGC North Am.* **28**(10), 874–878 (2010).
J.V. Hinshaw, *LCGC North Am.* **28**(11), 952–958 (2010).

System Operation

The steps to follow for restoring an idle gas chromatograph and column to operating condition

Recently, I needed to use a split–splitless inlet, column, and flame ionization detection (FID) system that had been idle for more than a year. The gas chromatography (GC) system had been in continuous use for valved applications, but the entire time the inlet carrier gas controller had been disconnected from the carrier gas supply, and the column oven connections and gas inlets had been capped. The intended column — 20 m × 180 µm, 0.12-µm d_f methylsilicone fused silica — had been stored in its box with the inlet and outlet stuck into a septum. The GC instrument itself was apparently in excellent working condition, so I optimistically anticipated a quick install and performance checkout. Fortunately, that prediction proved accurate. Here are the steps that I followed.

Instrument Setup

My initial task was to setup the pneumatics, inlet, and detector. First, with the GC system powered on, I checked the carrier gas configuration for the split–splitless inlet. Although the set column dimensions did not match the column I would use, the basic configuration would allow carrier to flow to the inlet once a supply was connected. I also made sure that carrier gas leak detection was disabled. I planned to purge the pneumatics initially and did not want the system to shut off the flow. I then double checked that the inlet and FID heaters were turned off and also turned off the detector and pneumatic controllers that had been in use.

Pneumatics

Next, I turned off the GC system power, allowed its zones to cool, removed the existing columns, and capped off the detector and carrier gas source that had been in use. I then removed the interconnecting tubing at the gas switching valves while making a note of how they were connected. The new application would require oven temperatures of up to 300 °C, well above the maximum limits for the gas sampling valves, so I disconnected the valves from their actuators and removed them as well.

In my next step, I inspected the gas tanks. I found suitable gas purities: 99.9999% research-grade helium carrier gas, zero grade air with <1 ppm total hydrocarbons, and high-purity 99.998% hydrogen. The carrier-gas regulator was a stainless steel diaphragm, high-purity dual-stage device, and the fuel gas regulators were brass dual-stage types. Moving down the installed copper gas lines, I found a suitable set of multistage gas filters that were in apparent good condition with little-to-no indicated filter exhaustion.

I turned off the carrier gas at the tank, moved the carrier-gas supply over to the pneumatic controller for the split–splitless inlet system, but did not tighten the connection completely, and capped the carrier-gas connection that had been used for the valved application. While making the carrier-gas connection, I noted that the existing tubing and ferrules appeared to not have been overtightened or scratched and that the nut screwed onto the fitting smoothly with no binding.

Before fully tightening the new carrier-gas connection, I turned the gas on at the tank and allowed some helium to purge through the line. This would protect the upstream filters by removing the air that had inevitably diffused in while the tubing was disconnected. Of course, any additional air present in the pneumatic controller would enter the line as well, so after tightening the fitting one-quarter turn past finger tight I immediately turned on the GC system and set a split flow of 50 mL/min at a 10-psig (70-kPa) inlet pressure.

I also turned on the air and hydrogen supplies, verified that the regulator output pressures were correct, and then enabled the FID fuel gas flows and checked that they were set to the correct values as well, according to the instrument manual.

After I was satisfied that the gas lines were purged sufficiently, I turned off the gas flows at the instrument pneumatic controllers and then closed the tank valves to commence a gross leak check. After 10 min, I turned the tank valves back on one at a time and observed any motion of the high-pressure gauges on the pressure regulators. An observable change in the high-pressure gauges that is greater than the wiggle produced by lightly tapping the gauges may indicate a serious leak that requires further investigation. I saw no discernible movement, so I proceeded to do a fine leak check of the hydrogen and helium lines with a leak-check device. On its high-sensitivity setting, the leak-checker probe picked up a small leak at the hydrogen filter fitting, but I was able to seal it completely by tightening the fitting one-eighth turn. Otherwise, I would have chosen to cut the tubing an inch shorter and remake the fitting with a new nut and ferrules instead of tightening the leaking fitting further.

Figure 1: Inlet pressure as a function of column length for a series of column inner diameters. Carrier gas: helium at 120 °C. Average linear velocity: 40 cm/s. Column outlet at atmospheric pressure.

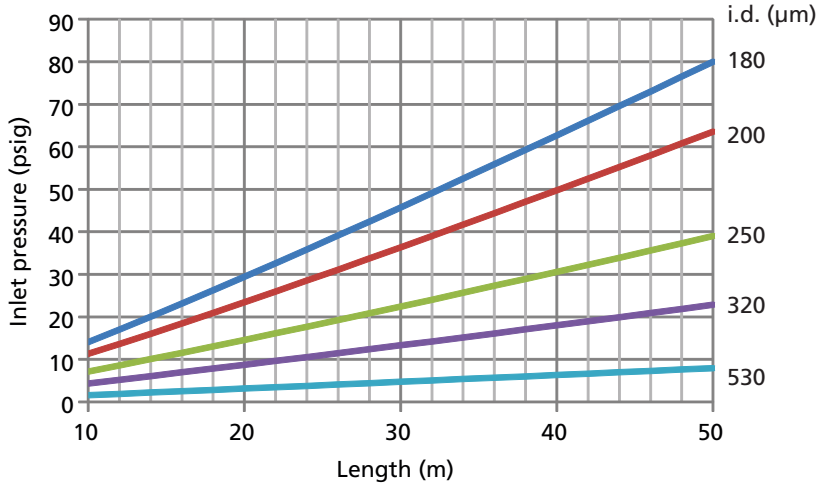

Figure 2: Unretained peak at 40 cm/s setpoint. Column dimensions: 20 m × 180 µm; carrier gas: 29.4 psig helium at 120 °C.

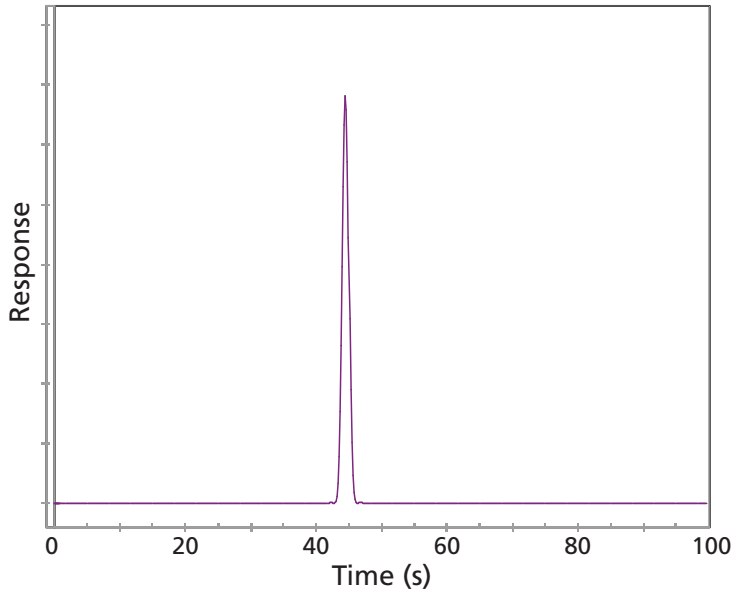

At this point, the instrument had been powered on for the better part of an hour, so it was time to zero the pressure transducers, which need some time to stabilize after powering on. The largest drift error in the pressure transducers is their zero reading. Span errors normally are not corrected, as that would require a very accurate (and expensive) external gauge, and in doing so one would be just as likely to introduce errors as to correct them.

Following the procedure in the manual, I turned off the gas supplies and allowed the line pressures to decay to zero, which took another 10 min or so. Then I accessed the pneumatic zeroing section of the instrument firmware and set the zeros. I finished by turning the gas supplies back on.

Inlet and Detector

I had to assume that someone might have fiddled with the components during the year of idle time, so after turning off the instrument power again I proceeded to check the condition of the inlet and detector. I like to wear lint-free gloves while handling inlet and detector parts, but I've used tweezers or pliers (gently) as well.

Although there was nothing apparently wrong with them, I removed and replaced the inlet septum, liner, and inner seals. While the inlet was disassembled I checked the column connection for bits of ferrule and the inlet cap for pieces of septum. Then I reassembled the inlet with new parts.

I removed the detector top, electrode, and collector tube from the FID system. They were clean enough so I simply put them back. The upcoming performance check would bring out any problems in that area. I also checked the FID fitting in the oven to make sure the inner passageway was clear. Before the next step, I sealed the FID oven connection with a blank graphite-vespel ferrule.

Then it was time to check the FID fuel gas flow calibration. I attached a digital flowmeter, recently calibrated, to the FID tower outlet and enabled the air flow first. The flow was within a few standard cubic centimeters of the set point, so I turned off the air flow and turned on the hydrogen flow. After remembering to switch the flowmeter to its hydrogen scale, I found the flow to be close to the set point as well. If this instrument had makeup gas flow for the FID system (which it did not), then I also would have checked that flow rate at this point. I made sure that the hydrogen flow was turned off before continuing.

When I have new inner parts in an inlet, I like to bake it out before installing the analytical column. This step will remove much of the inevitable contamination from the inlet. I installed an old 250-µm i.d. column I had on hand for such purposes, turned on the GC system, and set the carrier gas to 10 psig and 200 sccm of split flow. I did not connect the column outlet. After verifying that the split vent flow was present and calibrated, I checked around the inlet seals and column fitting for leaks. Then I set the inlet

Figure 3: Experimental data points with theoretical pressures and velocities: (a) length = 18.75 m, i.d. = 180 µm; (b) length = 19.25 m, i.d. = 183 µm; (c) length = 19.25 m, i.d. = 180 µm; pressure correction of +1.75 psi applied. In each case, the experimentally measured pressure–velocity data match the theoretical line.

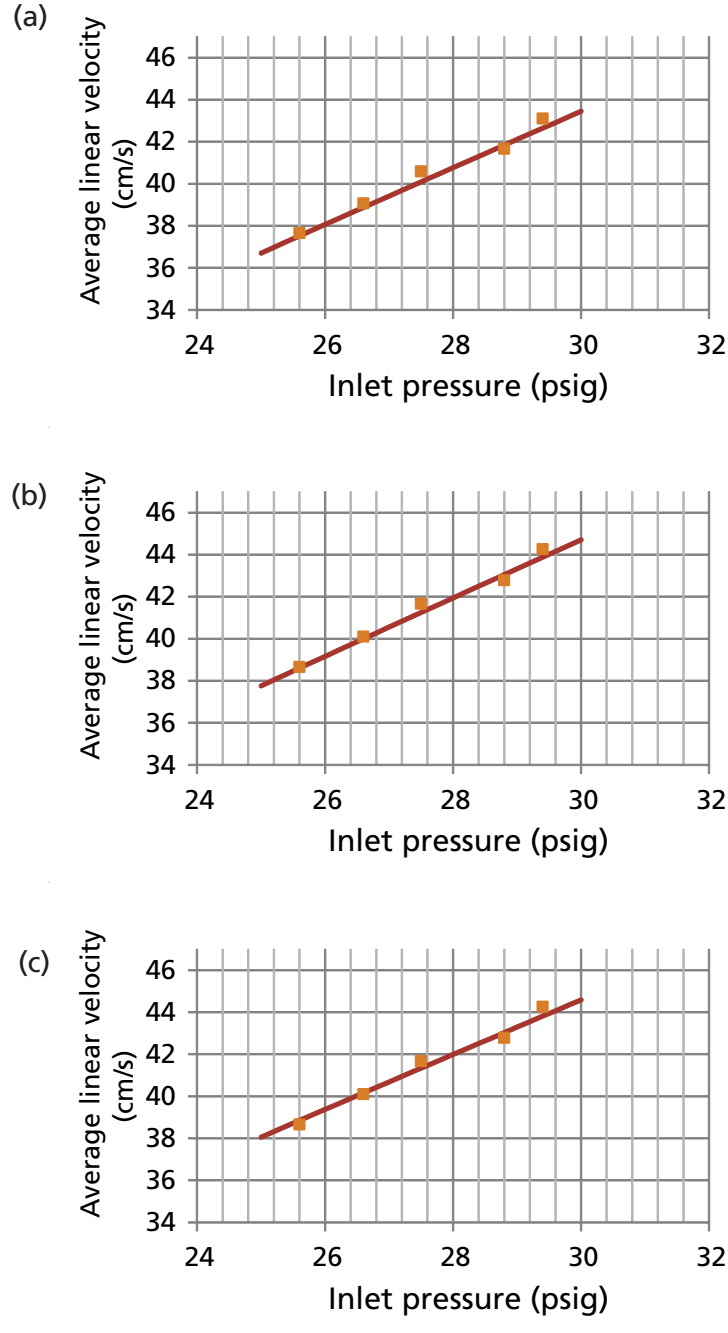

temperature to the maximum application temperature plus 20 °C — 300 °C in this case. The inlet was a programmable temperature device, so it heated up quickly. I set the GC oven to the bakeout temperature of the column to be installed later, also 300 °C, allowed the oven to stay there for 10 min, and then cooled the oven and inlet back down.

Naturally, since this oven had not been heated that high in quite a while, I had to assure some of my coworkers that no, there was no fire or electrical short — that the burning smell was normal and that I was ok. It was a great way to find out who's watching out for their colleagues.

Column Installation and Checkout

With the inlet baked and cooled, I was ready to install the analytical column. Like most used fused-silica GC columns, this one would be somewhat shorter than the originally specified length written on the box. I measured the approximate average coil diameter and counted the number of turns of column on its cage to check the length and get an estimate of how much was left: This came to 35 turns at a 17.5-cm diameter, for an estimated length of 19.25 m.

It is important to know the column dimensions because electronic pneumatic control systems calculate pressure, flow, and velocity on the assumption that the analyst has entered the correct dimensions. To the extent that the column dimensions are incorrect, the operating conditions also will be erroneous. Large errors, such as operating a 250-µm i.d. column with the pneumatic system set for a 320-µm i.d. column, should become obvious in short order, but smaller discrepancies might not be seen as clearly. I entered the column box dimensions, with a length of 20.0 m, an internal diameter of 180 µm, and a film thickness of 0.12 µm, to find out what the effects of incorrect column dimensions would be.

The thin stationary film would not contribute significantly to the pneumatic operation, but it's a good idea to be in the habit of always entering all of the column dimensions whenever installing a column. I also checked that the carrier gas was set to helium and that the split mode was set to flow control, not split ratio mode.

Using new ferrules, I installed the column at the inlet. Keeping the same 10 psig inlet pressure, I then turned on the inlet carrier gas and double checked for column flow by putting the column outlet into an autosampler vial that was half-filled with distilled water. The presence of bubbles revealed carrier flow. I then connected the column outlet to the detector. After a moment or two, I leak-checked the column inlet connection. There were no problems there.

Figure 4: The first two column bakeouts. Programming rate: 10 °C/min from 50 °C initial temperature. Final temperature: 300 °C. Subsequent temperature programmed baselines were similar to the second bakeout (green chromatogram).

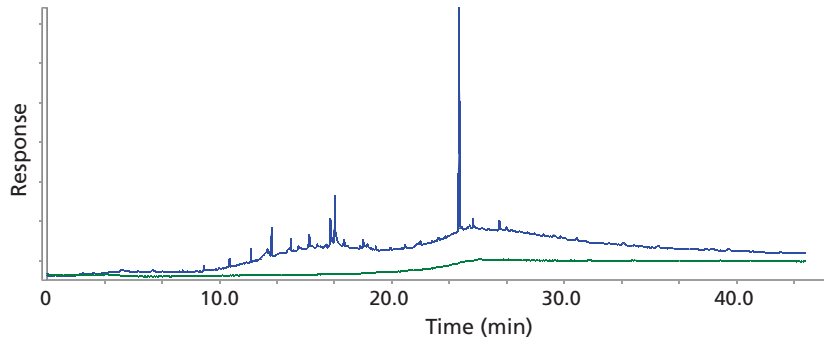

Figure 5: Nonpolar capillary column test mix. Column temperature: 110 °C; average linear velocity: 40 cm/s. Peaks: 1 = 2-octanone, 2 = *n*-decane, 3 = 1-octanol, 4 = 2,6-dimethylphenol, 5 = *n*-undecane, 6 = 2,6-dimethylaniline, 7 = *n*-dodecane, 8 = *n*-tridecane. Peak 8 measures 4380 theoretical plates/m, or a plate height of 230 µm.

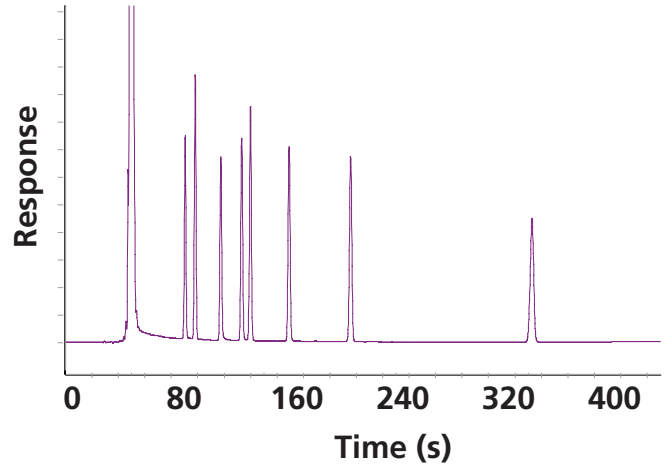

I activated the FID system, set the temperature to 300 °C, and allowed it to heat until the temperature exceeded 150 °C. Then I turned on the hydrogen and air flows and gave the ignite command through the keypad. In a moment, I heard the short pop of flame ignition. I double-checked for a flame by holding a cold wrench horizontally over the FID exit to observe some water condensation. The FID signal level had risen as well, verifying that the flame was staying lit.

Verifying the Column Dimensions

With the column installed, flame lit, and carrier flowing, it was time to verify that the pneumatic controller had column dimensions that were close enough to provide accurate readings of flow and velocity. I set the oven to 120 °C and entered a linear velocity of 40 cm/s. As the oven stabilized, the inlet pressure settled to 29.4 psig (202 kPa), and I was ready to inject some methane.

I chose to use the average linear velocity as my metric because this value is easily measured with sufficient accuracy. Column flow could be used instead, but that would require comparably accurate measurement of low flows, around 1 mL/min for the present column, which is very difficult to achieve even if the column is removed from the detector.

I set up a short, 2-min run on the data-handling system and injected 10 µL of 1% methane in nitrogen to capture the unretained peak time and shape. Figure 1 shows the result. The methane peak is symmetrical and the baseline noise is quite low. On closer examination, the noise appeared to be comparable to that found in previous chromatograms on this instrument, so I did not concern myself with it. This result signifies that the system is tight, with no serious detector leaks or poor electrical connections, and that the inlet system and column are free of obvious obstructions or misconfigured connections. A tailing methane peak would indicate a problem in the inlet liner or column connection areas, or possibly blocked or incorrect makeup gas flow at the detector.

However, the calculated average linear velocity from the 44-s unretained peak time was 45.5 cm/s for the nominal 20-m column length, not the set value of 40 cm/s. Although this approximately 10% error is not huge, it is instructive to consider possible sources for the discrepancy. Errors of this sort will result if the column length or diameter, the oven temperature (as it affects the carrier gas viscosity), or the pressures are not conveyed accurately to the electronic pneumatic system.

Theoretical equations can be used to calculate the range of inlet pressures required to produce an average velocity of 40 cm/s with helium at 120 °C, for example, with varying column lengths and internal diameters. I used a spreadsheet for this, to produce the family of curves illustrated in Figure 2. The curve for a 20 m × 180 µm column passes through our pressure setpoint of 29.4 psig (202 kPa) as expected, yet the measured average velocity was greater than 40 cm/s. A GC pressure–flow calculator application (1) also can be used to examine the effects on flow and velocity of changing column dimensions. Interested chromatographers can read more about the theoretical calculations on an external website (2).

The initial unretained peak measurement and velocity calculation implied that either the inlet pressure drop was

greater than its set level, the column was shorter than the entered 20 m, the column internal diameter was slightly larger than the set value of 180 µm, or the oven temperature was miscalibrated.

The oven temperature was the least likely culprit. This GC system had been temperature-calibrated in the past three months, and an error of 10 °C would only change the viscosity, and thus the velocity, by less than 2% anyway. I wasn't too concerned about the temperature.

I already knew that the column was shorter than its original 20 m: How much shorter would it need to be to achieve the desired 40 cm/s from the electronic pneumatic system? To answer this question, I measured a series of unretained peak times across a range of pressures that I guessed would cover the true 40-cm/s operating point. Because the average velocity is a function of the length as well as the pressure, I used a spreadsheet to calculate the theoretical linear velocities as a function of the pressure and length. The theoretical predictions matched the measured data well when the column length was 18.75 m, as shown in Figure 3a. When the applied column length diverged much from 18.75 m, then the experimental data could no longer be said to match the theory.

I had measured the column length at 19.25 m. Is a 50-cm error in the length reasonable given how it was measured? With 55 cm/turn, a one-turn counting error would account for it. Or, an error of 0.5 cm measuring the coil diameter would produce a similar effect across the 35 turns. After working up these data, I retrieved the column and carefully remeasured the coil diameter and turns count, twice. However, the results were the same. The coil diameter appeared to be accurate to about 0.15 cm; the turns count was unchanged. Thus, it seemed that the column length alone was insufficient to account for all of the effects on linear velocity.

The column internal diameter also could play a role in the linear velocity discrepancy. Pressure drops are sensitive to the square of the diameter, so a small difference in the actual versus nominal diameters also could be in play. I set the theoretical column length to 19.25 m, and calculated that the inner diameter would need to be around 185 µm to achieve a 40 cm/s average velocity at an inlet pressure of 26.6 psig. Figure 3b shows this result. I also noted that if the column length were assumed to be 20 m, the inner diameter would have to be about 188 µm to account for the observations.

Generally, column internal diameters are quite accurate. They are controlled to tight specifications by precision laser gauges during column tubing production. One publication cites the internal diameter of similar tubing as 180 ± 5 µm (3), so an upper limit of 185 µm is not out of reach.

Finally, perhaps the inlet pressure was not calibrated, although it had been zeroed. Would a positive or negative pressure offset account for the measured velocity data? Yes, indeed. A positive offset of +1.75 psia (12 kPa) would be sufficient, as shown in Figure 3c, to produce the velocity effect in lieu of a larger column internal diameter. Modern pressure control systems should be capable of much more accurate operation, but perhaps this 10-year-old GC system was not up to the challenge.

From the above considerations, the most likely source of error in the matching of linear velocity set point and measurement was the analyst; in this case, myself. It was highly suspicious that exactly one turn of column coil length would account for the results, yet the column length seemed to have been measured accurately. Some combination of pressure, diameter, and length could be operating together, but simplicity, and the fact that columns are trimmed routinely, led me to conclude that compensating by entering an adjusted column length was the best way to bring linear velocity in line.

Short of uncoiling the column and measuring how many tiles it spans on the laboratory floor — which I did once a long time ago and failed to recover a neatly coiled column in one piece after someone stepped on it — the next best way to measure length is the turns method; just be careful to get an accurate turn count and diameter measurement. Count twice and inject once. Use the measured length as a starting point, then use a GC pressure–flow calculator to figure out an adjusted length to enter into the pneumatic controller so that the velocity readout is reasonably accurate.

If large adjustments seem necessary to align the measured and displayed linear velocities, then question the entire setup and be prepared to review each step of the system configuration and installation process.

Bakeout and Performance Test

Finally, I baked the column out at 300 °C (twice), and then ran a polarity test mixture to gauge its performance. Figures 4 and 5 show these results, which were well within expectations with the exception of the slightly tailing solvent peak. This tailing peak had the look of a minor detector problem typical of chlorinated solvents, such as the methylene chloride in use here, but since the analytes were not affected I chose to ignore it. With a well-characterized column up and running, I was ready to proceed to the application itself.

Conclusion

Restoring an idle capillary inlet and detector system can be straightforward if the inlet, column, and detector were sealed and stored properly. Conducting fairly simple pneumatic and hardware checkouts and leak checks before attempting to run any chromatograms will hasten the restoration process. Given that few capillary columns come back to the GC oven with the same length, as originally stated on the box, be prepared to spend a little time adjusting electronic pressure control settings if accurate flow and velocity readings are desired.

References

(1) See the Agilent pressure–flow calculator application and software at http://www.chem.agilent.com/en-US/Support/Downloads/Utilities/pressureflowcalc/Pages/default.aspx.
(2) http://wiki.hrgc.com.
(3) S. Griffin, *LCGC North Am.* **20**(10), 928–938 (2002).

How to Cite This Article:
J.V. Hinshaw, *LCGC North Am.* **30**(3), 224–232 (2012).

Air Leaks

What happens when air leaks into the carrier-gas line, and what to do about it

Leaks are anathema to chromatographers. Wasteful of ever more scarce and expensive gas or liquid mobile phase, leaks have been blamed for detector noise, baseline instability, inaccurate flow calibration, column degradation, and potential explosion or toxicity hazards. Conventional laboratory wisdom states that any leak is to be avoided, even trace leaks that don't materially affect flow measurements or gas consumption.

In gas chromatography (GC), the gas supply lines are bathed in a mixture of 78% nitrogen, 21% oxygen, and 0.9% argon, plus some water and a smattering of trace-level gases, which is to say, room air. Room air can flow or diffuse past a leaky fitting, diaphragm, or seal into regulators, supply lines, and inlets, so the potential exists for oxygen and water to enter carrier-gas lines through poorly made-up fittings, permeable regulator diaphragms, or leaking septa. The result: expensive, high-purity 99.9999% carrier gas gets downgraded to something less pure. Good laboratory practice calls for careful attention to fittings, checking for leaks with high-sensitivity electronic leak detectors, the use of appropriately rated high-purity gas regulators and valves, and regular septum and inlet seal replacement. Installation of gas filters that trap oxygen, hydrocarbons, and moisture is highly recommended as a stop-gap measure against the traces of contamination that might make their way into the carrier gas despite all the other precautions.

The effects of gas impurities are relative to the sensitivity of the instrumentation and columns to the contaminants. Some capillary GC columns — the "wax" types for example — can degrade rapidly in the presence of sub-part-per-million ($<10^{-6}$ volumetric concentration) levels of oxygen when operated at elevated temperatures. Certain detection methods, such as flame ionization detection (FID), are not sensitive to air contamination but they are quite sensitive to the hydrocarbon content of their fuel gases. Other detection methods, such as discharge ionization detection (DID), are exquisitely sensitive to contaminants. Gas sampling valves for very high sensitivity work can require various purge arrangements that flood the valves with carrier gas externally as well as internally to prevent even the slightest influx of air into the active valve passageways. The fact that it is necessary to resort to such measures clearly demonstrates the significance of extremely small gas leaks.

For this chapter, I measured the extent of air incursion against some extremely large gas leaks. I had to resort to very large leaks to see any effects because I was not using very sensitive equipment, just a conventional GC system with thermal conductivity detection (TCD) that can only detect down to several parts per million of air in helium.

Contamination or Leakage?

Carrier gas leaks and poor quality carrier gas can yield similar problems: They both cause contaminants to enter the column and detector. In the course of investigating issues with carrier-gas quality I wondered, how much air does enter a carrier-gas line against a detectable leak? The concept of air flowing into a fitting against the outward flow of exiting carrier gas seems counterintuitive; could this really happen?

Recently. I investigated what apparently were several locally sourced cylinders of contaminated ultrahigh-purity (UHP) helium that had been installed on a group of process analyzers in a remote area halfway around the world from my location in the western United States. A little experimentation in the laboratory with a test analyzer quickly revealed that the helium carrier gas in the remote analyzers seemed to contain something like 1000 ppm of nitrogen, orders of magnitude more than the 1 ppm or less that should have been present. But this finding left open the question of the origin of the contaminating nitrogen: Was it in the cylinders themselves or had it entered the carrier gas downstream from the cylinders due to a leak or a defective seal? All the evidence pointed to poor quality cylinders. The rates of gas consumption were normal, no leaks were evident when examined during a service visit, high-purity gas regulators had been installed, and the side effects of the contamination were very similar for each of the analyzers. If leaks were involved, then it seemed unlikely that the leakage would be nearly the same for each of the three independent analyzers with their own individual carrier-gas tanks.

A quick experiment further exonerated any reasonable leakage as a source of nitrogen contamination. With no carrier-gas filters in place, I simply loosened the carrier-gas bulkhead fitting on the laboratory test system until a large leak could be detected with

Figure 1: Nitrogen calibration with chromatograms of 0–500 ppm N_2. Peaks: 1 = injection disturbance, 2 = oxygen, 3 = argon, 4 = nitrogen, 5 = unknown. Conditions are described in the text.

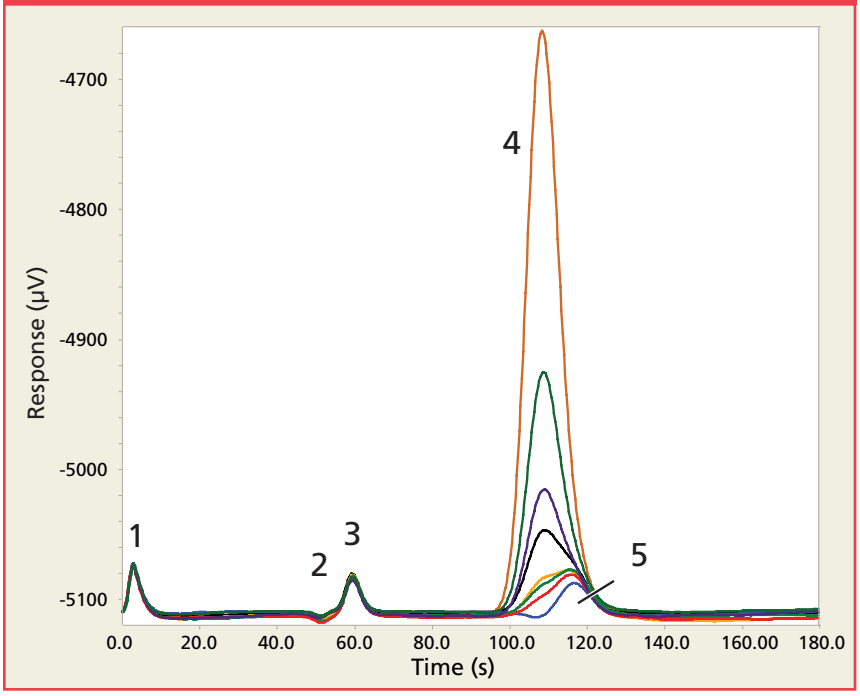

Figure 2: Chromatograms showing the effect of air leaks with increasing orifice sizes: blue, zero leakage; yellow, 0.5-mm ferrule; black, 0.8-mm ferrule; purple, 1/16-in. ferrule; green, 1/8-in. ferrules; orange, open tee fitting. Peaks: 1 = injection disturbance, 2 = oxygen, 3 = argon, 4 = nitrogen, 5 = unknown. Conditions are described in the text.

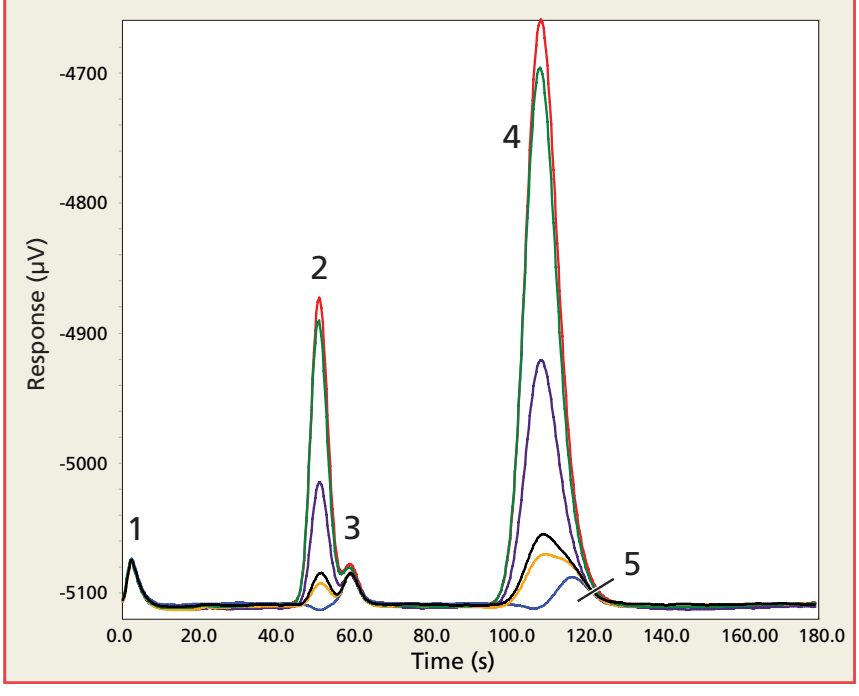

a handheld electronic leak detector set on its low sensitivity range. This had no effect on the chromatography and did not produce the characteristic baseline-upset symptoms of high levels of nitrogen contamination. I went even further and loosened the carrier-gas fitting enough to cause an audible hiss as the gas escaped. At this leak rate, the cylinder pressure dropped from around 2300 psig (15.8 mPa) to 2150 psig (14.8 mPa) in 2 h, which would have emptied the tank in short order. Yet, no noticeable effects were seen in the chromatography. The resulting nitrogen contamination in the carrier, if any, was nowhere near 1000 ppm.

This left me wondering: Just how much air does move into the carrier-gas stream against an outgoing leak, and how much does the air influx depend upon the size of the leak? As I thought about it, I recalled an inadvertent but similar result from an earlier "GC Connections" installment (1). At that time, I had been looking into carrier leaks inside a GC system and had found an incorrectly assembled and leaky bulkhead fitting at the back of the instrument. Repairing the fitting had no effect on the chromatography back then, either. In that case, the leak was found in the column inlet.

Measuring Leaks

At this point, I decided to quantify how much air (as nitrogen) would leak into the gas line as a function of the size of an orifice from which gas was free to leak out and air to flow back in against the leak. I installed a freshly conditioned 2.0 m × 1.0 mm 100/120 mesh micropacked molecular sieve 5A column (Supelco) on a PerkinElmer AutoSystem XL GC system along with a six-port rotary gas-sampling valve (VICI) and 1.0-mL sample loop, all configured for conventional gas sample injection. The sample gas source was connected to the sample loop input through a 1/8-in. tee fitting followed by a solenoid on–off valve, and I connected 1-m length of 0.5-mm i.d. stainless steel tubing to the rotary valve sample output to stop air from diffusing back up into the

Figure 3: Nitrogen concentration as a function of leakage orifice area, from the chromatograms in Figure 2.

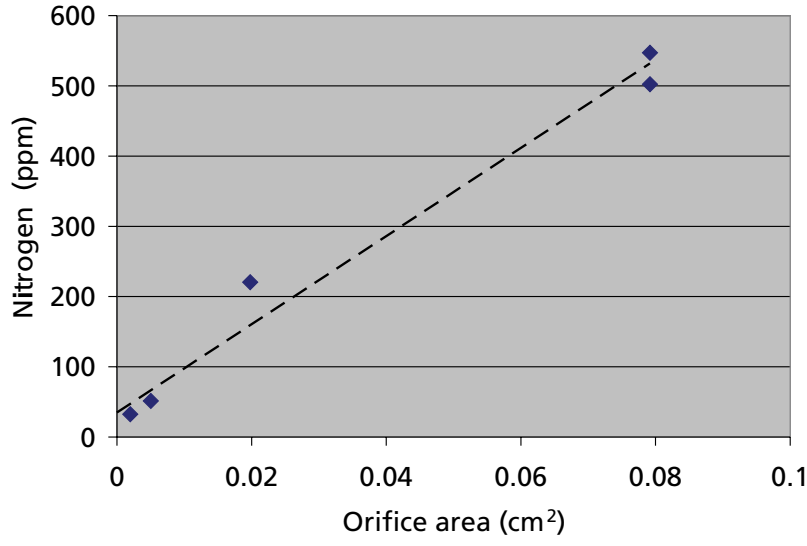

valving and loop while the loop pressure was allowed to decay to room pressure, before injection. The thermal conductivity detector was set to its highest sensitivity. A cylinder of UHP helium carrier gas already had been set up on the GC system. The oven temperature was set to 50 °C and the carrier pressure to 40 psig, which gave a column flow rate of 11.2 sccm. The system was stabilized at these settings for 12 h before proceeding.

Next, I calibrated the detector response by feeding the output from an Environics model 4020 gas dilution system to the sample loop via a back-pressure regulator and gas take-off arrangement at a constant pressure of 30 psig. This produced a flow rate through the sample loop of around 500 sccm, which was more than sufficient to flush the connecting tubing and loop thoroughly. A second cylinder of certified UHP helium carrier gas was mixed by the dilution system with varying flows of 5000 ppm (±2%) N_2 in UHP helium from a gas standard cylinder (Scott Gas) to produce N_2 concentrations of zero and then seven concentration steps from 6 to 500 ppm. Figure 1 illustrates the calibration chromatograms across the injected range. The calibration curve had a linear regression coefficient of r^2 = 0.9991, with a zero intercept of +320 µV-s due to the constant unknown peak under N_2, as can be seen in Figure 1 (peak 5). This extra peak may be krypton but I had no ready source with which to confirm its identity. The oxygen and nitrogen peaks were slightly negative with the pure UHP helium diluent, which indicated that the carrier gas contained roughly the same amounts of these gases as the diluent gas. With TCD, it was not possible to better discern such low levels.

Then, to determine the effects of varying the size of a major leak on nitrogen levels in helium carrier gas, I replaced the gas connection from the dilution apparatus with a connection to a third UHP helium cylinder using a different regulator as well. First, I obtained a few chromatograms with no leaks present, which were identical to the zero-level chromatograms from the gas dilution system. Then I performed some initial leak tests with the helium source at 40 psig (350 kPa). I created various leaks by loosening the sealed 90° side connection on the tee fitting in stages. First, the fitting was loosened just enough to get a significant reading on the helium leak detector. Then it was opened a bit more, and then finally to the point of creating an audible leak. Yet, none of these chromatograms were significantly different than those obtained with no leaks. This finding is consistent with the observation on the process analyzer in the laboratory that creating a large leak did not affect the chromatography in comparison to knowingly introducing contaminated carrier gas. It also is consistent with the earlier observation that a leaking bulkhead fitting was not the cause of characteristic baseline disturbances on a different system.

The Mythbuster Test

Most of the readers of *LCGC North America* are familiar with the "Mythbusters" television show. The hosts address an urban legend by attempting to recreate conditions that lead to the alleged effect or result. If they cannot recreate the desired effect as documented, then they resort to evermore extreme conditions and test to the point of a dramatic failure.

At this point, having shown in three different ways that detectable levels of air — detectable with TCD, that is — did not seem to enter the carrier-gas line against some small and some extreme leaks that might normally be encountered in the laboratory, I wanted to find some conditions, any conditions, under which detectable levels of air would enter a gas line against an outgoing leak. I decided to perform a "Mythbuster" test, although there was no dramatic exploding endpoint, just the possibility of an empty gas cylinder and a little more helium in the laboratory air.

To do this, I first reduced the tank regulator output from 40 psig down to 4 psig (35 kPa), not only to reduce the outgoing helium flow, but also because I was about to install some very large holes in the gas line, which at the higher pressure would have emptied the tank in a matter of hours. Besides being very noisy. I opened the side fitting on the

tee completely and measured the nitrogen level in the line. Then I installed open 1/8-in. stainless steel ferrules with an open nut to hold them in place. After measuring this nitrogen level, I replaced the ferrules with a series of 1/8-in. fitting sized capillary column graphite–Vespel ferrules having increasingly smaller hole sizes: 1/16-in., 0.8-mm, and 0.5-mm i.d. The nitrogen level was measured after 10 min of flow with each orifice size. Figure 2 shows the chromatograms from this series. Note the oxygen peak, absent from Figure 1, which confirms the presence of air.

These results are shown in Figure 3 as a plot of the observed nitrogen concentration against the approximate area of the orifice openings. A fairly linear relationship was found, considering that I didn't actually measure the orifice sizes and I didn't take any steps to ensure that the pressure was the same for each ferrule — it could have changed due to differing pressure drops across the tubing from the regulator to the openings as the flows changed. In any case, these results clearly show that air does flow back against an outward helium leakage flow. I didn't attempt to extrapolate to smaller orifices and flow rates, but there is a strong implication that even much smaller leaks can allow significant traces of air to enter a carrier-gas stream. It should be possible to measure them with a more sensitive system. Bear in mind that here we are discussing levels well above 1 ppm, while true trace-level gas analyses run down to the parts-per-trillion (10^{-12} volumetric concentration) level where even the best seals can start to look like large leaks and where leak-free operation imposes an entirely different regimen.

Conclusion

I didn't run the tests to a point of dramatic failure — emptying an old tank of helium is pretty benign. But, this simple demonstration underscores the necessity for leak-free connections, high-purity regulators, and rigorous gas filtration for any GC system that is running at high sensitivities or using capillary columns. Air leaks are not the only source of contamination, of course, and especially with current trends in helium availability and cost, more attention to helium cylinder quality in some remote locations is warranted.

Reference

(1) J. Hinshaw, *LCGC North Am.* **21**(1), 34–40 (2003). (http://chromatography-online.findanalytichem.com/lcgc/data/articlestandard//lcgc/052003/45060/article.pdf)

How to Cite This Article:
J.V. Hinshaw, *LCGC North Am.* **27**(11), 984–988 (2009).

Preventive Maintenance

How to avoid crises through periodic maintenance of your GC system

Periodic maintenance is the mainstay of keeping laboratory instruments running at the peak of performance. Analysts can avoid many problems by proactive evaluation, repair, and replacement of critical system components on a regular basis. The alternative of allowing contamination to build up, syringes to wear out, or septa to leak only results in increased down-time compared to planned maintenance outages. Unplanned maintenance and repair is not predictable and in my experience, most such incidents occur at the worst time.

Periodic maintenance procedures fall into two categories. First are those that should occur on a regular basis, for example, every six months. Second are those for which the frequency is determined by system usage characteristics (for example, to be performed every 200 injections) and usually set by the type of sample and its level of contamination; dirtier samples impose more frequent maintenance on syringes, inlets, and the column entrance or retention gap. This chapter presents some recommended maintenance intervals and related suggestions for a number of the major components of a gas chromatography (GC) system. Table I lists maintenance items and both regular intervals as well as sample-based intervals. The suggestions in this article are not intended as a set of rules to be followed rigidly. Rather, the information should be considered as a partial list of items that should be subject to periodic maintenance. Each laboratory has different requirements, not all of which appear here. It's a good idea to review maintenance procedures because laboratory requirements and usage patterns change over time.

Regular Timed Maintenance

Procedures that should be performed on a regular time basis include such simple things as straightening up the laboratory area, dusting behind instruments, archiving instrument logbooks, or defragmenting disk drives. Most laboratories run a fairly clean operation, although I've seen some remarkable exceptions in my travels. Usually, some dirt and grime will accumulate beneath instruments and computers or become trapped around gas lines and electrical cords. More seriously, a buildup of dirt on instrument cooling air intake vents and filters, on internal cooling fans and heat sinks, and around computer components eventually can compromise instrument operation. While it's simple enough to clean around the outside of instruments and computers, opening up the panels and clearing out the internal dust is another matter. Doing so exposes the inside of the instrument or computer to potential harm from static discharges, especially as found at the end of a vacuum cleaner hose, and also exposes untrained personnel to high voltages that might be present, in some cases even if the power is off and the AC line unplugged. Such operations are best left to trained service persons.

Certain pieces of equipment should be checked — and checked functionally where appropriate — every so often. Gas tank regulators, external gas lines and their fittings, gas generation equipment, and the types or grades of gas in use should all be examined at least every three months. Verify that the carrier and detector gases are of the correct identity and grade. I once came upon a laboratory where the helium carrier gas cylinder had mistakenly been replaced with a nitrogen cylinder (in the United States both have the same style high-pressure fitting), which resulted in some apparently mysterious chromatographic behavior until the problem was discovered.

Leaks can develop in gas fittings as they are opened and resealed — for example, while replacing in-line gas filters. And speaking of gas filters, it's a good idea to label new filters as they are installed with the date and type of filter being put into use. Check each in-line gas union with a high sensitivity helium leak detector — they also react to hydrogen. Such a device won't pick up leaks in nitrogen or air lines, but I don't recommend using any kind of liquid leak solution. In these cases, a pressure drop test will reveal any gross leaks. Turn off the air or nitrogen carrier, detector, or make-up gas flow at each connected gas chromatograph, then close the gas tank high-pressure side regulator valve and wait 10–20 min. When the high-pressure valve at the tank is reopened, observe whether the high-pressure gauge reading jumps upward significantly. If so, then there is a downstream leak somewhere. I sometimes will repressurize the lines with helium just so that I can use the helium leak detector to pinpoint such a leak. Just remember to reconnect to the correct tank when you are ready to put the instrument back into service.

Gas generation systems are easy to install but sometimes, especially when installed out of direct view,

Table I: GC system maintenance items and suggested performance intervals

Category	Item	Procedures	Interval (whichever comes first)	
			Regular Interval	Upon a Condition or Event
Instruments	Cleaning	External cleaning	Weekly	
		Internal cleaning	Twice per year, professionally	
	GC oven temperature	Calibrate	Annually	
	EPC	Pressure transducer zero	Every three months	
Gases	Regulators	Check regulator type		
		Leak check		
		Performance check	Yearly	
	Filters	Replace		After number of gas tanks specified by manufacturer, or when indicated
		Appropriate type of filter		When changing filter
	Fittings	Leak check		Whenever a seal is made
		Correct assembly; correct application of sealing tape		Whenever a seal is made
	Gas standards	Inspect certification	Every three months	Weekly when in use
		Replace		
	Gas tanks	Check remaining pressure	Every two weeks	Replace if pressure is <250 psig (1.7 MPa)
	Gas type and grade	Inspect	Every three months	When changing tanks
Autosampler	Operation	Inspect, test main functions	Monthly	
	Syringe	Inspect	Monthly	When starting a sequence or tray
		Leak test	Monthly	As dictated by sample contamination and residue
		Replace	Three months	When leaking or if plunger does not operate smoothly
Inlets	Septa	Replace		After 100 injections; With each inlet liner
	Liners	Replace		When contaminated; on performance loss; sample dependent
	Upper liner seal (o-ring)	Replace	Six months	With each inlet liner
	Lower liner seal ("Gold" seal)	Replace		After cleaning inlet; if lower seal is opened
	Split, column, and septum purge flows	Measure	Monthly	When changing operating conditions; after replacing liner or septum; after inlet cleaning or repair; after installing a column
Columns	Retention gap – precolumn	Replace		When contaminated; on performance loss; sample dependent
	Nuts and ferrules	Inspect, tighten		After first runs when new
		Replace		When replacing, reinstalling column or retention gap
	Performance	Measure with QA/QC sample or manufacturer's test mix	Weekly	After column or retention gap installation
Detectors	Combustion and makeup gases	Measure	Weekly	After gas tank change, change of set-point, or detector repair or installation
	Electrodes, optical window, flame jet	Inspect	Monthly	Upon detector disassembly
		Clean	Every six months	Loss of performance, noise, visible contamination
	Performance	Measure	Monthly	Part of suitability tests

they can be ignored for longer than desirable. I have seen several instances of gas generation equipment running with the "service required" and operational indicators facing the wall, presumably to get better access to the inlet and outlet fittings, so that it was impossible to see the status of the generator. Eventually, such situations will manifest themselves with increased noise and drift. It's preferable to check and perform the necessary maintenance in advance.

The high-pressure diaphragm in the dual-stage pressure regulators used in chromatography laboratories operates under a high stress level at the intermediate pressure stage of up to 500 psi (345 N/cm^2). With time and many pressure/flow changes during normal use the high-pressure diaphragm can suffer metal fatigue, as can the counter-spring. This gradual loss of performance can take years, but then again, I've seen many pressure regulators that must be more than 25 years old still in routine use in GC laboratories. Early symptoms of regulator degradation can be a loss of regulating ability, so I like to test regulators every year or so by turning off the gas at the regulator outlet valve and then disconnecting the supply tubing somewhere convenient toward the instrument. Then I gradually turn on the gas at the regulator outlet valve to increase the flow as I observe the pressure on the outlet gauge. As the flow rate increases, the outlet pressure should drop slightly but remain within 5 psi or so of a 90-psig (620-kPa) set-point for a high-quality, dual-stage laboratory regulator. Another sign of a problem is when the outlet gauge does not return to zero when the regulator is depressurized, or if the needle is bent. Such a broken regulator should be replaced immediately.

Pure inert gas supply tanks generally don't have an expiration date, but certified gas standards do. I sometimes will keep expired gas standards around for a quick test of a setup, but I always make sure that in-certification tanks are used when making quantitative measurements. The same goes for liquid standards. Also, any gas blending equipment in use will have a fixed expiration date for its accuracy certification and will need to be recalibrated regularly, usually once a year. Other equipment in use in the laboratory such as precision thermometers, voltammeters, and data-acquisition systems also require recalibration on a regular basis. GC oven temperatures sometimes drift out of specification over a long time period — more so on older instruments — and many laboratory periodic maintenance procedures call for checking and recalibration. Also, electronic pressure control (EPC) systems will require regular zeroing and accuracy checks as the electronic pressure gauges contained in them undergo normal aging and drifting.

Sample-Determined Maintenance Intervals

Beyond fixed maintenance intervals, some maintenance procedures should occur on the basis of how many injections have transpired and also in relation to the level of sample cleanliness. For example, septa develop leaks in proportion to the number of injections, while autosampler syringe barrels wear both with the number of fill–eject cycles and the level of sample contamination. Many of these items should be performed on a "whichever comes first" basis, and these have entries in both columns in Table I labelled "Regular Interval" and "Upon a Condition or Event."

Autosamplers include components in both categories. GC system operators should verify the basic mechanical functions of an autosampler on a regular basis by observing that the device runs smoothly, triggers no errors, and delivers expected levels of precision and accuracy. A sudden loss of performance in a GC system might be a symptom of a poorly functioning autosampler. Autosampler syringes, however, are subject to wear both as a function of how many fill–eject cycles occur plus how much residue is in the samples. Counter to intuition, a larger number of postinjection wash cycles can wear out a syringe in fewer total injections, if the sample contains nonvolatile residue that builds up inside the syringe barrel. Selection of the right rinse solvent can help increase syringe life significantly. Leak testing a syringe involves dismounting it from the autosampler, filling and emptying the barrel with a representative solvent while observing any bubble formation or leaks around the needle or barrel, and assessing the difficulty with which the plunger moves. If any doubt exists as to the condition of a syringe, it should be replaced.

Inlet septa don't degrade over time, but they can develop significant leaks fairly rapidly, often after as few as 100 injections. This depends strongly upon the type of syringe needle and whether automated or manual injections are performed. Inlet liners, on the other hand, are subject to degradation mostly from the buildup of sample residue that can interact with subsequent samples either chemically or by adsorption. Replacement intervals for liners run from one injection to thousands. I have come across a number of laboratories that perform little to no sample preparation of biological samples, thus finishing off one liner per injection, as well as others, in the business of checking highly pure solvents for impurities, where one liner can last for a very long time.

With elevated inlet temperatures, the o-ring seal at the top of the liner does degrade over time, so even in cases in which the liner itself is still fine, the seal should be replaced at least on a regular timed interval. In inlet systems with a lower metallic wafer seal, if the seal is interrupted for any reason, then it must be replaced because leak-tight metal-to-metal contact requires a pristine surface. It's also a good idea to double-check split vent and septum-purge flows after changing any injector parts or the column; that should be part of a normal method set-up procedure as well.

The column itself is subject to degradation resulting from sample injections as well as temperature programming. Dirty samples can deposit nonvolatile residues at the beginning of the column, which leads to increased column bleed, adsorption with associated peak tailing, and the potential breakdown of sensitive compounds in subsequent injections. Other column-degradation routes include oxygen in the carrier gas from poor supplies or leaking fittings. In any case, the damage is cumulative across multiple injections and temperature program cycles. Regular evaluation of column performance will track any degradation and provide a clear indication of when to change the column. A retention gap or precolumn in front of the analytical column will trap much of the sample residue so that trimming or replacing the retention gap section will restore much of the original column performance. However, a retention gap will do nothing to prevent thermal damage to a column.

Detectors also will degrade over time and as a result of the accumulation of column bleed byproducts. Symptoms include increased noise, reduced sensitivity, and higher offsets. Detector components such as flame ionization jets and collectors, photoionization and flame-photometric optical windows, and thermionic beads all require regular inspection, cleaning, or replacement as appropriate. And like inlet and column flows, analysts should check detector flows after performing any maintenance procedures in order to be sure that normal flow rates have been reestablished.

Spring Cleaning

Laboratories can benefit greatly from enacting regular maintenance procedures that are triggered by both timed intervals and by the sampling history of individual instruments. Initially, establishing a regimen for sample-based maintenance means monitoring the relationship between the number of injections, sample purity and type, and the changes in instrument performance that result. The initial effort can be well worthwhile and can help reduce instrument downtime as well as increase results quality. "Spring cleaning" really is not a good term to describe this process. It implies a once-yearly effort to clear out long accumulated dust and debris, while the concept discussed here is a proactive effort to establish regular and directed procedures that will prevent the "buildup" of performance-robbing conditions in laboratory gas chromatographs.

How to Cite This Article:
J.V. Hinshaw, *LCGC North Am.* **28**(3), 218–224 (2010).

Upgrading GC

Guidelines for upgrading your gas chromatography (GC) laboratory to use high-speed GC and generate your own gases

Technologies for laboratory analysis advance continuously, just as do computer technologies or transportation technologies. Small advances tend to occur fairly often while major new technologies appear less frequently. As new capabilities become available, laboratories must decide whether to acquire them or to defer and continue to use what they already have. Such decisions are reached by considering the roles and requirements of the laboratory, the short and long-term costs of the new technologies, new skills that laboratory workers may have to acquire, and the relative benefits and drawbacks of all of the changes.

Reasons and justifications for technology upgrades depend upon laboratories' current and future needs. While the benefits of new capabilities are easy to describe, what may not be so evident are the collateral requirements of implementing new technologies in the laboratory. For example, switching to hydrogen carrier gas generation eliminates the costs of carrier-gas cylinders and can yield faster speeds of analysis if hydrogen is not already in use, but the change also invokes some new safety requirements and procedures. This chapter discusses two related gas chromatography (GC) technologies and their impact on laboratory equipment and procedures.

Generate Your Own Gases

Installing carrier- and flame-gas generators is relatively easy, although there are some special considerations for hydrogen. The benefits of zero future gas cylinder costs plus no cylinder transport or demurrage charges yield an attractive return on investment (ROI), especially given the current high cost of carrier-grade helium. Zero-grade air generators are effective as well. The cost of detector-quality cylinder air is much lower than carrier-grade helium, but its "burn rate" is much higher at over 400 mL/min compared to a range of 50–250 mL/min for carrier gas with a split inlet system. Carrier-gas consumption can be reduced by up to 80–90% if a gas-saver pressure-control mode turns off split flow while the inlet is not actively in use. There is no corresponding saver mode for flame ionization detection (FID) air. A flame detector needs to stay lit and stable as long as there are pending analyses. The result is that much more FID air is used in the average laboratory than carrier gas.

Gas generators have limited flow and pressure ranges that cannot be exceeded. It's a good idea to acquire gas generators that exceed current flow requirements by 25–50% to allow for future expansion. Also, installing gas generators will create a new requirement for regular generator maintenance, although arguably this is less effort than it takes to haul cylinders in and out of the laboratory.

Hydrogen: Generation of hydrogen for carrier and fuel gas invokes some additional concerns. For the majority of GC applications, hydrogen carrier gas can be substituted for helium. The exceptions are for certain fixed-gas separations as well as for some detection methods, such as helium ionization detection (HID) and electron-capture detection (ECD), in which helium actively participates in the detection chemistry. Even in these cases, it is sometimes possible to apply helium as the makeup gas while using hydrogen as carrier gas, which at least will reduce helium consumption. As an alternative, most ECD systems will work with a 5% methane in argon makeup gas mixture, although sensitivities and relative responses will change compared to helium. Mass spectrometry (MS) detectors are generally compatible with hydrogen carrier; some reduced pumping efficiency as well as lower background ionization levels can be expected. Also, some extra attention to proper detector venting is called for when shutting down to avoid hydrogen accumulation inside the detector's vacuum chamber. MS detector manufacturers can provide detailed information about their specific products. For standard GC separations with FID, hydrogen carrier is an attractive choice because the same hydrogen source also can be used for the FID fuel gas. See reference 1 for some additional frequently asked questions about hydrogen carrier gas.

Switching to generated hydrogen carrier gas is a two-step process. First, if not already using hydrogen, install a tank of high-purity hydrogen, or use the existing FID hydrogen tank if it's pure enough, and validate performance with the new carrier. The column pressure settings will be different. Lower inlet pressures are required for the same average carrier-gas linear velocities, while the optimum velocity for hydrogen is 10–20% higher than for helium. A flame ionization detector requires a constant flow of hydrogen fuel, which means electronic pneumatics will be needed

Together, we can reduce your carbon footprint by decreasing energy usage.

One factor that users of compressed gas should consider when selecting a supply method, is the effect that production and delivery of gas has on the environment. Extraction, fractional distillation, delivery and handling of compressed gas cylinders or dewars requires a great deal of energy and has a direct impact on the environment. The energy employed by these processes generates a significant amount of CO_2, which is believed to have an unfavorable effect on climate change.

Users of compressed gases may wish to consider an alternative source, such as an in-house gas generator which will produce far less CO_2 and is a much less expensive source of gas over time. To learn more, visit **solutions.parker.com/noco2.**

aerospace
climate control
electromechanical
filtration
fluid & gas handling
hydraulics
pneumatics
process control
sealing & shielding

Parker Balston

ENGINEERING YOUR SUCCESS.

solutions.parker.com/noco2

Cabinet Cascade

Often, a seemingly simple decision to deploy a new capability will lead to a cascade of other changes that are required to support and enable the new technology. I experienced such an effect a few years ago when deciding to replace a 20-year-old inefficient kitchen refrigerator with a new energy-efficient model. I made some measurements and determined that the small storage cabinet above the current refrigerator was exactly 5/8 in. too low to clear any of the new models and thus had to be moved higher or removed entirely. But, repositioning the one cabinet would have made it uneven with the cabinet next to it, a progression that reached all the way around the room. If all the wall-mounted cabinets had to be moved, perhaps it was time to replace them instead. But the new upper cabinets would not match those under the countertops, so they should be replaced as well. And if replacing those, then new countertops were in order, too. A new countertop would require a new sink . . . . At this point, I realized that I was considering an expense of many times the cost of the new refrigerator, let alone the time, effort, and inconvenience of a kitchen makeover. Today, the small kitchen cabinet sits in the garage. Maybe I'll use it to store tools.

to maintain flow when the column is temperature programmed. Run the carrier pneumatics in constant-flow mode if possible, and establish a constant total FID hydrogen flow.

After the new carrier-gas and detector settings have been validated, then consider switching from cylinders to a gas generator. From a cost point of view, it might be easier to justify a new hydrogen generator if several GC systems can be converted to hydrogen carrier at once.

Beyond considerations for method parameters, using hydrogen carrier gas will invoke some concerns for the potential burning or explosion hazards. A cylinder of flammable gas represents three distinct hazards. First, the very high pressure in any gas cylinder is a physical endanµgerment to personnel if not well understood and handled correctly. Second, the cylinder is very heavy and can present a lifting or falling hazard. Third, hydrogen is flammable and becomes explosive when mixed with air at concentrations between the lower and upper explosive limits of 4–74% by volume. A fully pressurized A-size cylinder at 2600 psig (18 kPa) contains nearly 8 m^3 of gas when expanded to room pressure. In a small 20 × 30 × 10 ft (6 × 9 × 3 m) laboratory, the lower explosive limit (LEL) of hydrogen could be reached if the entire contents of a cylinder were released at once. However, this extreme occurrence is very unlikely to take place by accident.

Using a hydrogen generator to produce carrier and fuel gas relieves concerns for the release of a tankful of hydrogen — the generators store only a small amount of hydrogen at any time. Small amounts of hydrogen can be released into the laboratory from split vents or during column installation. For peace of mind, it might be a good idea to install a hydrogen sensor near the ceiling of the laboratory. I have one such sensor in my laboratory that gets tested — loudly — once in a while when I change the carrier gas to hydrogen and purge the carrier-gas lines. But I experiment with different carrier gases much more often than would a production laboratory.

Modern GC systems include some safety features that address hydrogen concerns as well. Any laboratory that is considering hydrogen carrier is strongly urged to use an instrument with an electronic pressure control system that limits the flow of hydrogen carrier gas and detects and shuts off the flow under leakage or out-of-bounds conditions. Today's GC systems feature explosion-safe ovens that, upon the extremely rare occasion of hydrogen accumulation and ignition, will contain the overpressure safely inside the oven. Hydrogen leak detector accessories are available for GC ovens as well.

Increase Speed of Analysis with High-Speed GC

Going to faster speeds of analysis with GC doesn't always require a new or upgraded instrument, but not all existing instruments are suitable. It all depends on how fast a separation is required. A modest increase of two to four times shorter retentions using conventional capillary columns with inner diameters of 200 µm or greater can be achieved quite reasonably on a wide range of conventional laboratory instruments. Very high speeds can achieve separations that previously needed 10 min or longer in less than 1 min, but such a feat requires significant equipment upgrades or complete replacements. Pushing peaks from a column at high speeds places demands on autosamplers, inlets, detectors, and data-handling systems that existing equipment might not be able to handle adequately. Newer GC systems incorporate high-speed autosampler injection modes, appropriate inlet designs, and fast data acquisition speeds that encompass the requirements for high-speed operation up to a point. Specialized micro GC systems or dedicated rapid column heating accessories are required to go even further.

Making the decision to go to higher speeds is just the start of what can be an extended method development and validation exercise. A high-speed capable instrument is a platform on which to deploy a suitable column and method. It might be able to inject and record very narrow peaks while ramping up the column temperature at impressive rates, but without the necessary separation method, it will not deliver the desired results.

Generally, faster linear velocities and higher temperatures or temperature program rates, as well as reduced column lengths and inner diameters, will achieve a given separation in less time. This is attractive when considering whether to purchase additional GC systems for the laboratory, and when faced with an increasing sample load. Alternatives such as adding a temporary work shift or contracting to an

outside laboratory might be good intermediate solutions but in the longer term, increasing the sample throughput capacity of the laboratory is going to be more cost effective. But the route to achieving higher analysis speeds can be difficult to traverse.

Certainly, hydrogen carrier gas is effective for faster GC separations because it is less viscous than helium and so produces higher linear velocities at the same pressures. The higher "speed limit" for hydrogen becomes important when pushing longer columns with narrower inner diameters to yield faster separations — speeds of analysis are faster as inlet pressures approach their maximum values. Shifting to higher analysis speeds isn't a simple matter of cranking up the inlet pressure, however. A number of other parameters and considerations come into play in the GC fast lane.

First and foremost, the peaks of interest must be resolved sufficiently under a new set of conditions. If the separation is isothermal, and if there is extra resolution to start with, then achieving higher speeds is relatively simple. Even when increasing pressures to operate well above optimum velocities, in such situations, enough room between the peaks is available to produce adequate resolution at the higher speeds. All of the peaks move in proportion to an increase in velocity; their separations (α-factors) do not change, assuming the stationary phase is the same..

Another approach to high-speed separations involves going to smaller column inner diameters. Reducing the column inner diameter while still operating at close to the optimum velocity will produce more theoretical plates and correspondingly narrower peaks, and it will increase the resolution. Then the chromatographer can choose to crank up the inlet pressure and increase linear velocities away from the optimum, sacrificing the increased resolution of the narrower inner diameter column for more speed.

Shifting peaks: Things get more complex with temperature-programmed separations, or when increasing isothermal temperatures. The elution times of all of the peaks decrease while the relative positions of dissimilar peaks shift as the temperature program rate increases, which also will happen when increasing the temperature of an isothermal separation. This behavior stems from the different ways in which solutes interact chemically with the stationary phase as temperatures change. In a temperature-programmed run, modifying the pressure settings, or even changing from constant pressure to constant flow mode, also will change relative peak positions. In this case, solutes experience slightly different temperatures as they move through the column more rapidly, while the oven temperature program profile is unchanged.

Reducing the column inner diameter is another approach to higher speeds, as already mentioned. However, with temperature programming there exists the possibility that peaks will shift in relation to each other if the column phase ratio (β) is not maintained while reducing the inner diameter. For example, a 530-µm i.d. column with a 1-µm stationary phase film has a phase ratio of

$$\beta \approx r_c / 2d_f = 265 \qquad [1]$$

In a 250-µm i.d. column, with a potential of about a 1.4× higher theoretical plate count, the corresponding available film thickness for the same approximate phase ratio would be 0.5 µm. If the phase ratio is not kept about the same when changing column inner diameter, then dissimilar peaks in a temperature-programmed separation will again experience relative retention shifts.

This sensitivity of the separation of dissimilar peaks to changing column dimensions, temperatures, and pressure conditions makes it necessary to optimize and validate any significant changes in an effort to achieve higher speeds. Simulation software such as Agilent's Method Translation Software (2) (Agilent Technologies) can significantly reduce the time and number of experiments required to reach a desired combination of speed and resolution from which to start formal method validation.

Achieving satisfactory results with high-speed GC, then, requires both the right kind of host equipment and a suitably developed and validated separation. Modest speed increases often are possible with existing equipment, but truly high-speed separations will require a commitment to obtaining the equipment and developing the methods. Crossing the bridge from conventional to high speeds can invoke more work than expected, but high-speed separations can be well worth the extra effort when laboratory requirements demand them.

The Cascade Effect

In both cases presented here — advancing laboratory operations by switching to gas generation or by transitioning to higher-speed analyses — the decision to improve laboratory capabilities will produce a successful outcome only if laboratory personnel fully consider the implications of the changes and perform the necessary predeployment tasks to ensure that the desired goals can be achieved. Changing to hydrogen carrier gas requires careful planning and consideration for both the potential added hazard as well as appropriate GC method changes. Upgrading to high-speed GC is a great idea, but performance requirements can necessitate the purchase of additional or replacement equipment. In any case, upgrading laboratory technologies is neither simple nor easy, but the results can be well worth the effort.

References

(1) J.V. Hinshaw, *LCGC North Am.* **26**(11), 1100–1109 (2008).
(2) Available for download with no cost at http://www.chem.agilent.com/en-US/Technical-Support/Instruments-Systems/Gas-Chromatography/utilities/Pages/gcmethodtranslation.aspx.

How to Cite This Article:
J.V. Hinshaw, *LCGC North Am.* **28**(1), 34–41 (2010).